

UC Davis

UC Davis Previously Published Works

Title

Whole Genomes Inform Genetic Rescue Strategy for Montane Red Foxes in North America.

Permalink

<https://escholarship.org/uc/item/47f6z9bj>

Journal

Molecular Biology and Evolution, 41(9)

Authors

Quinn, Cate

Preckler-Quisquater, Sophie

Buchalski, Michael

et al.

Publication Date




2024-09-04

DOI

10.1093/molbev/msae193

Peer reviewed

Whole Genomes Inform Genetic Rescue Strategy for Montane Red Foxes in North America

Cate B. Quinn ^{1,2,3,*} Sophie Preckler-Quisquater,¹ Michael R. Buchalski ²
Benjamin N. Sacks ^{1,4}

¹Mammalian Ecology and Conservation Unit, Veterinary Genetics Laboratory, School of Veterinary Medicine, University of California, Davis, Davis, CA, USA

²California Department of Fish and Wildlife, Wildlife Genetics Research Unit, Wildlife Health Laboratory, Sacramento, CA, USA

³National Genomics Center for Wildlife and Fish Conservation, USDA Forest Service, Rocky Mountain Research Station, Missoula, MT, USA

⁴Department of Population Health and Reproduction, School of Veterinary Medicine, University of California, Davis, Davis, CA, USA

*Corresponding author: Email: catherine.quinn@usda.gov.

Associate editor: Joanna Kelley

Abstract

A few iconic examples have proven the value of facilitated gene flow for counteracting inbreeding depression and staving off extinction; yet, the practice is often not implemented for fear of causing outbreeding depression. Using genomic sequencing, climatic niche modeling, and demographic reconstruction, we sought to assess the risks and benefits of using translocations as a tool for recovery of endangered montane red fox (*Vulpes vulpes*) populations in the western United States. We demonstrated elevated inbreeding and homozygosity of deleterious alleles across all populations, but especially those isolated in the Cascade and Sierra Nevada ranges. Consequently, translocations would be expected to increase population growth by masking deleterious recessive alleles. Demographic reconstructions further indicated shallow divergences of less than a few thousand years among montane populations, suggesting low risk of outbreeding depression. These genomic-guided findings set the stage for future management, the documentation of which will provide a roadmap for recovery of other data-deficient taxa.

Key words: conservation genomics, genetic rescue, inbreeding, genetic load.

Introduction

In small populations, inbreeding depression can inhibit population growth, thereby perpetuating inbreeding and accelerating population decline, a causal chain known as an “extinction vortex” (Gilpin 1986). In turn, the deliberate translocation of breeding adults from another population can improve mean fitness, increase population growth, and elicit a “genetic rescue” from inbreeding depression (Whiteley et al. 2015). While the short-term benefits of genetic augmentations are concrete and generalizable (Frankham 2015), the long-term consequences are comparatively uncertain and context-dependent (Bell et al. 2019). Possible adverse outcomes include outbreeding depression (Edmands 2007), homogenization of locally distinct gene pools (Harris et al. 2019), exacerbation of existing inbreeding depression (Kyriazis et al. 2021), or fitness increases that are weak or ephemeral and drain resources from competing conservation actions (Hedrick and Fredrickson 2010). The information necessary to address these uncertainties has been prohibitively expensive or logistically unfeasible to obtain through traditional field approaches for many populations. Consequently, genetic rescue is a management

tool that is frequently mentioned in conservation strategies and seldom implemented (Fitzpatrick et al. 2023).

Genomic sequencing has the potential to aid management decisions by rapidly filling information gaps regarding the risks and benefits of genetic rescue (Segelbacher et al. 2022; Fitzpatrick et al. 2023). Most fundamentally, genomic data can be used to quantify runs of homozygosity (ROH), which are identical tracts of DNA inherited from both parents (Kardos et al. 2016; Ceballos et al. 2018). Evidence of recent inbreeding can be juxtaposed with sequence-based reconstructions of long-term effective population size to identify vulnerable populations in need of genetic rescue. Once need is established, most hazards associated with implementation relate to the source population providing the novel genetic variation. Traditionally, outbreeding depression has been the primary concern, stemming from intrinsic incompatibilities or adaptive divergence between donor and recipient genotypes (Edmands 2007; Frankham et al. 2011). A newer concern is the potential for translocated individuals to introduce new deleterious recessive variants (Van Oosterhout 2020): if augmentations fail to initiate rapid population growth, these variants may unite in

Received: March 12, 2024. Revised: August 07, 2024. Accepted: September 03, 2024

Published by Oxford University Press on behalf of Society for Molecular Biology and Evolution 2024.

This work is written by (a) US Government employee(s) and is in the public domain in the US.

Open Access

homozygous form, exacerbate inbreeding depression, and increase extinction risk (Kyriazis et al. 2023; Pérez-Pereira et al. 2022). In both cases, risk is predicated on divergent demographic trajectories of donor and recipient populations. Chromosomal rearrangements and co-adapted gene complexes typically require hundreds to thousands of generations in isolation to evolve (Frankham et al. 2011). The total abundance of deleterious alleles is also shaped over long timescales through mutation and purifying selection, but can be redistributed over shorter time scales through drift and inbreeding (Robinson et al. 2023). Genomic characterization of demographic histories and deleterious variation provide the means to navigate this complex landscape of relative risk and benefits but has not yet been widely applied in management.

Certain populations of red foxes (*Vulpes vulpes*) endemic to the mountainous regions of the contiguous western United States are currently being evaluated for genetic rescue (Sierra Nevada Red Fox Conservation Advisory Team 2022). Montane red foxes are a lineage that diverged from other North American red foxes during the last glaciation and historically have been associated with the upper montane life zone of the western United States (Aubry et al. 2009; Sacks et al. 2010). Today these foxes are managed as three different subspecies (Fig. 1a). The Rocky Mountain red fox (*V. v. macroura*) is relatively abundant and well-connected with no corresponding protective status; whereas, the two subspecies associated with the Pacific mountain ranges of Washington (Cascade red fox; *V. v. cascadenis*) and Oregon and California (Sierra Nevada red fox; *V. v. necator*) are restricted to a few isolated, high-elevation populations (Quinn et al. 2022). Accordingly, each of the remnant red fox populations in the Pacific mountains has some degree of conservation status. They are state-endangered in Washington, state-threatened in California, federally endangered in the Sierra Nevada of California, and a “conservation strategy species” in the Oregon Cascades. Most recently, the US Fish and Wildlife Service was petitioned for a second time to federally list the populations in the southern Cascades of Lassen, California, and Oregon (Center for Biological Diversity 2024). Abundance is unknown for most of these populations, but the Lassen population is believed to comprise fewer than 30 individuals (Sierra Nevada Red Fox Conservation Advisory Team 2022).

Basic data on the ecology, demography, and evolutionary history of montane red foxes is sparse, to the point that a lack of information on which to base management decisions is itself frequently cited as a threat (Perrine et al. 2010). Paradoxically, no clear extrinsic limitations to growth have been identified (Sierra Nevada Red Fox Conservation Advisory Team 2022) and seemingly suitable high-elevation habitat is abundant (Quinn et al. 2018; Green et al. 2023). Yet for all four populations in the Pacific mountains, distribution is restricted and genetic diversity and effective population sizes have been estimated to be extremely low (Quinn et al. 2022). Together these

observations suggest that small population size itself may be limiting growth (i.e. genetic allee effects; Luque et al. 2016), in which case genetic rescue may be a requisite to jumpstart demographic recovery. Alternatively, early naturalists report that montane red foxes historically existed at low densities in fragmented distributions, in which case small effective sizes may instead be a long-term attribute of montane red fox populations that is intrinsically linked to their distinct ecology and history. In this case, extended periods of isolation could buffer contemporary populations from the most severe fitness consequences of recent inbreeding and carry greater risk for management actions that artificially facilitate gene flow.

A better understanding of the demographic history of montane red foxes and its genomic consequences is needed to guide an augmentation strategy for rescuing small Pacific mountain populations. Most immediately, the California Department of Fish and Wildlife is currently considering implementing genetic rescue of the Lassen population. Top candidate source populations include the Oregon Cascades, part of the same Sierra Nevada subspecies, and a population from eastern Oregon, belonging to the Rocky Mountain subspecies (Sierra Nevada Red Fox Conservation Advisory Team 2022). The most critical information gaps for evaluating the suitability of implementing genetic rescue for the Lassen and other isolated populations include the severity of inbreeding, the historical baseline that genetic rescue would be seeking to restore, and the deeper evolutionary relationships of montane subspecies. To address these gaps, we sequenced whole genomes of all available tissue samples from small Pacific mountain populations and compared them to representative samples from other regions of North America. Our objectives were, first, to reconstruct the long-term history of the montane lineage of red foxes, with an emphasis on identifying when contemporary populations became isolated from each other. Second, we sought to elucidate the extent to which low genetic diversity reported in past studies arose from recent declines or long-term small effective sizes, and third, to compare the total, expressed, and potential loads of deleterious variation across montane populations. We then applied our findings toward evaluating the suitability of using genetic rescue as a conservation tool to minimize extinction probability of isolated Pacific mountain populations, with particular attention to the Lassen population.

Results

Sampling and Population Structure

We sequenced 28 whole genomes from the four recognized subspecies of the montane lineage, including four small and isolated populations in the Pacific mountains (Washington Cascades [WAC], Oregon Cascades [ORC], Lassen Cascades [LAS], and the Sierra Nevada [SN]), a broader regional population in the Rocky Mountains [RM], and a phenotypically and ecologically distinct subspecies in the Sacramento Valley of California (SV) (Fig. 1a). To contextualize within-lineage

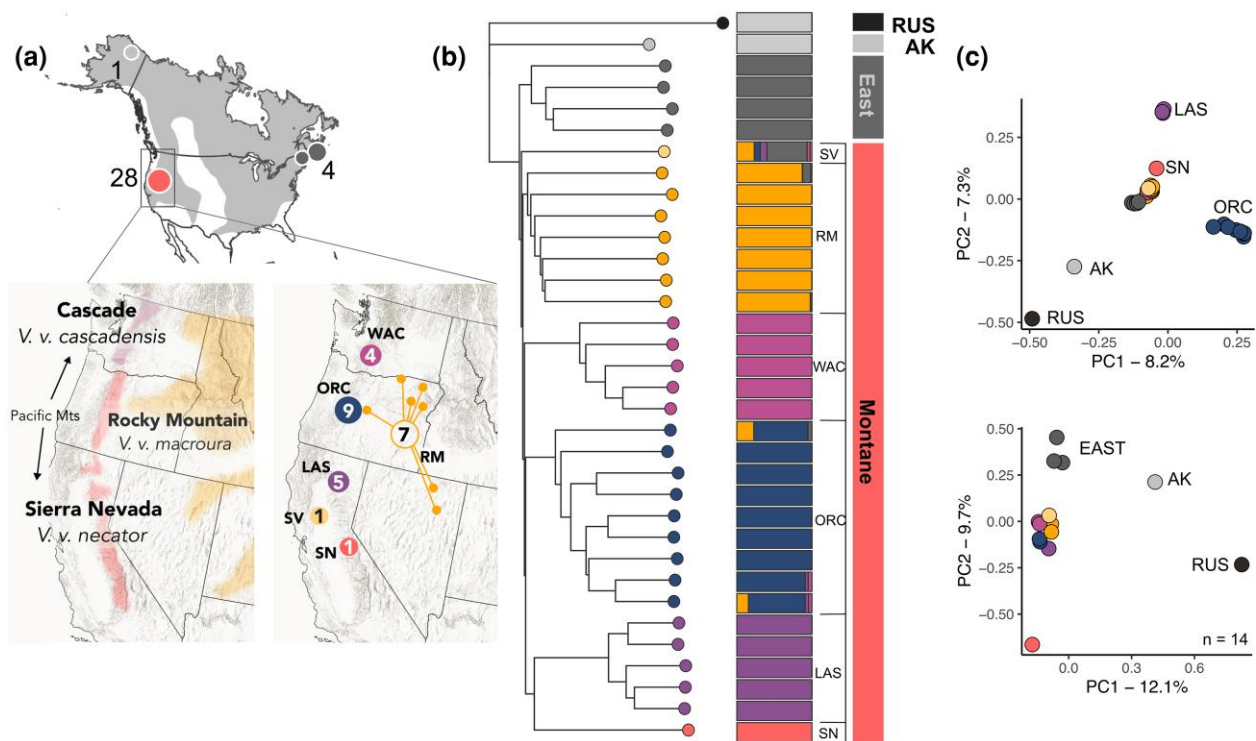


Fig. 1. Red fox sampling and population structure. a) Montane subspecies designations and sampling localities for 34 red foxes selected for whole genome resequencing (Russia not shown). Left map shows historical ranges of recognized subspecies and right map indicates approximate location and sample size for each population. b) Neighbor-joining dendrogram based on identity-by-state distances and genetic clustering inferred from Admixture at $K = 7$. c) PCA of all sequenced samples (top) and for samples reduced to 1 or 2 unrelated individuals per population (bottom). WAC, Washington Cascades; ORC, Oregon Cascades; LAS, Lassen Cascades; SV, Sacramento Valley; SN, Sierra Nevada; RM, Rocky mountains.

comparisons, we sequenced four samples from the eastern lineage, one from Alaska, and one from Russia. We used a chromosome-level arctic fox (*Vulpes lagopus*) reference genome (Peng et al. 2021) to map, genotype, and annotate sequences (supplementary table S1, Supplementary Material online), yielding an average depth of coverage of 17 \times and \sim 16 million bi-allelic SNPs.

We first characterized contemporary patterns of genetic structure in North America, with a focus on contextualizing the strong substructure of montane populations observed in other studies (e.g. Quinn et al. 2022). A neighbor-joining tree based on identity-by-state supported basal divisions between previously described refugial groups (east, montane, Alaska) in North America (Aubry et al. 2009; Sacks et al. 2010, 2018), as well as monophyly of subspecies and populations within the montane group (Fig. 1b). However, short internal branches indicated shallow absolute differentiation generally, and among montane populations specifically. In contrast, admixture analysis and PCA showed strong substructure within the montane group, with Pacific mountain populations (LAS, ORC, and WAC) being first to differentiate at lower K values in admixture analyses, as well as significant drivers of genetic variation in the PCA (Fig. 1b and c, supplementary figs. S1 to S3, Supplementary Material online). Kinship coefficient estimates within Pacific mountain populations suggested multiple first- and second-order relationships,

particularly in LAS, ORC, and WAC (supplementary fig. S4, Supplementary Material online). While the elevated kinship in WAC could be due to overrepresentation of a family group collected from a narrow portion of the known range, the samples from LAS and ORC were collected across their respective ranges and believed to accurately reflect population-level kinship. When we down-sampled to ≤ 2 unrelated samples per montane population, all montane samples except the SN individual collapsed into a single group (Fig. 1c). Together, these results suggest that the strength of substructure within the montane lineage is primarily driven by drift due to recent small effective sizes rather than long-term divergence.

Long-term Demographic History

We estimated temporal trends in effective population size (N_e) over the last two glacial periods using multiple sequential Markovian coalescent (MSMC2; Schiffels and Wang 2020). According to MSMC2, North American red foxes maintained large effective sizes through most of the Wisconsin glaciation and became demographically independent from Eurasian red foxes 300,000 to 400,000 year ago (Fig. 2a). This timeframe aligns with first appearance of red foxes in the North American fossil record and mitochondrial findings (P  w   and Hopkins 1967; Aubry et al. 2009; Statham et al. 2014; Sacks et al. 2018). However, the

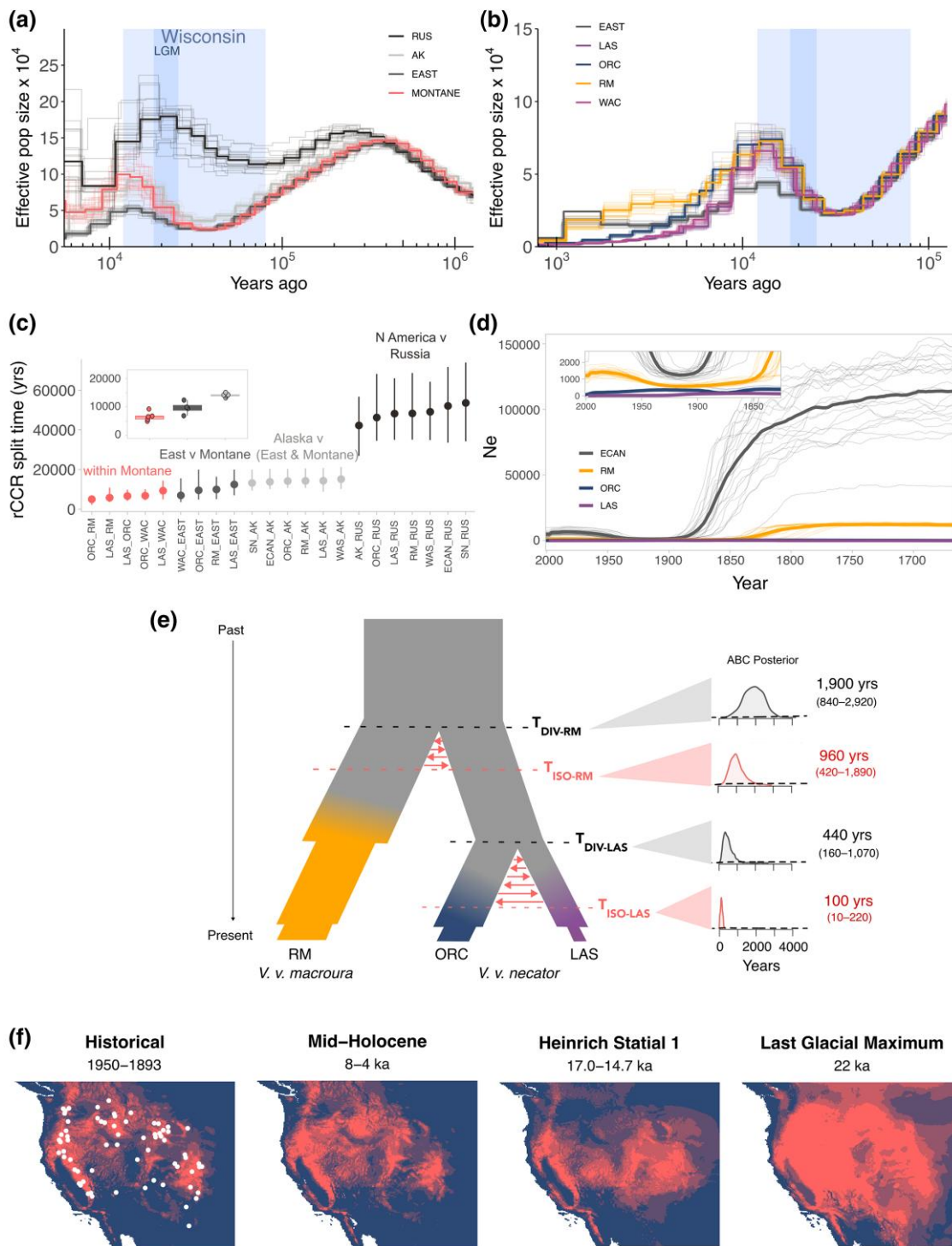


Fig. 2. Demographic history. Inferred changes in effective population size over time using MSMC2 with a) one sample per population and b) two samples per population. c) Estimated divergence time based on the rCCR estimated with MSMC2. d) Temporal N_e over recent time periods reconstructed with GONE. Thin lines are 20 independent replicates of 50 k SNPs per chromosome and thick lines are the replicate average. e) Three-population ABC model with posterior density estimates (median and 95% highest posterior density) for time of initial population division (T_{DIV}) and time of isolation (T_{ISO}) between the RM, ORC, and LAS populations. f) Climatic niche of montane red fox predicted from the location of 68 museum specimens (white points) and projected to past climates.

relative cross-coalescent rate (rCCR), an index of divergence based on the ratio of between- to within-population coalescence rates, suggests a more protracted and recent division (Fig. 2c, supplementary fig. S5, Supplementary Material

online). Continental populations did not majorly differentiate until 35,000 to 70,000 year ago, which supports considerable secondary gene flow across the Bering land bridge prior to its submergence 11,000 ago (Jakobsson et al. 2017).

Within North America, all three refugial lineages showed similar patterns of N_e through most of the Pleistocene, albeit with different magnitudes of N_e fluctuation (Fig. 2a and b). Effective sizes appear to have declined throughout the Holocene (ca. last 12,000 years), reflecting increasing coalescent rates from either reduced population sizes or changing structure (Mather et al. 2020). The rCCR point estimates for divergence for North American groups were closely overlapping, with the Alaska group diverging first (13,000 to 15,000 years ago), followed by separation between the eastern and montane groups (7,000 to 12,000 years ago), and most recently, divisions within the montane group (5,000 to 9,000) (Fig. 2c, supplementary fig. S5, Supplementary Material online). Divergence estimates younger than 10,000 years ago approach the resolution limit for MSMC2 analyses based on only 2 to 4 haplotypes per population (Schiffels and Wang 2020). Additionally, sporadic phasing errors are prone to breaking up identity-by-descent tracts, which disproportionately influence recent coalescence (Mather et al. 2020). Nonetheless, MSMC2 clearly identified the major genetic divisions within the montane group as younger than 10,000 years.

Short-term Demographic History

We used patterns of linkage disequilibrium (LD) in the program GONE (Santiago et al. 2020) to estimate trends in N_e over recent centuries (Fig. 2d). In contrast to long-term N_e , where eastern red foxes showed a lower N_e relative to the montane lineage for most of the late Pleistocene, historical trajectories indicated that N_e of the eastern group exceeded that of the montane group by several orders of magnitude throughout the modern era. Despite the different scales, both eastern and RM red foxes exhibited steep declines in the early 1800s, followed by modest recovery around 1950. In comparison, estimates of N_e for the Pacific mountain populations (ORC and LAS) stayed consistently low. This “flatlining” of N_e into the distant past is likely an artifact of their extremely small contemporary N_e , as drastic recent declines tend to erase the LD signature of older demographic events (Santiago et al. 2020).

Time of Isolation

We used approximate Bayesian computation (ABC; Beaumont et al. 2002) to infer the demographic history of montane populations during the Holocene, focusing on patterns of divergence and isolation for three populations: RM from *V. v. macroura*, ORC and LAS from *V. v. necator* (Fig. 2e). We chose these populations for their larger sample sizes and relevance to potential genetic rescue efforts of LAS. Simple pairwise models of divergence-with-migration (supplementary fig. S6, supplementary table S2, and Supplementary Material online) suggested that gene flow continued between ORC and LAS (within subspecies) until only about 20 years ago, whereas gene flow between these populations and RM (between subspecies) ceased around 600 years ago (supplementary fig. S7, supplementary table S3, and Supplementary Material online). We then pooled

posteriors from three-population models with two different patterns of stepping-stone migration that were equally favored (supplementary fig. S6, supplementary tables S4 and S5, and Supplementary Material online). These more realistic models indicated a median divergence time for RM from the ancestral ORC and LAS population ($T_{\text{DIV-RM}}$) of 1,900 years with gene flow maintained up until $\sim 1,000$ years ago ($T_{\text{ISO-RM}}$; Fig. 2e, supplementary fig. S8, supplementary table S6, and Supplementary Material online). Median divergence between ORC and LAS within subspecies ($T_{\text{DIV-LAS}}$) occurred around 500 years ago, with continued migration until a century ago ($T_{\text{ISO-LAS}}$). These estimates align with current recognized taxonomic classification, showing LAS and ORC as connected populations prior to historical declines, whereas separation of these populations from RM, recognized as different subspecies, predates the colonial period commonly used as a restoration baseline (Thorpe and Stanley 2011). Fundamentally, estimates across models consistently supported montane subspecies as evolutionarily young relative to one another. Accounting for cross-validation error rates (23% for $T_{\text{ISO-RM}}$, 44% for $T_{\text{DIV-RM}}$; supplementary fig. S9, Supplementary Material online), upper bounds of 95% highest posterior densities conservatively predict basal divisions within the montane group as no older than 4,000 years, with significant gene flow persisting until at least 2,300 years ago.

Climatic Niche Reconstruction

We reconstructed the climatic niche of montane red foxes using museum records that predated the most recent severe declines. Projections into past climates indicated a greater area of suitable habitat during the Last Glacial Maximum (LGM, 18,000 to 22,000 years ago) compared to present, paralleling the larger effective sizes and weaker structure of montane red foxes we inferred from MSMC2 (Fig. 2f). Climatic conditions that resemble the contemporary montane climate were both more expansive and continuous during the LGM. As the glaciers retreated, this climatic niche became increasingly fragmented and restricted to the footprint of the western cordilleras, until the mid-Holocene (ca. 6,000 years), when it stabilized to resemble the contemporary climate. Despite a clear trend toward increased fragmentation during the Holocene, the model suggested greater historical connectivity in the early 1900s than evidenced by the discrete genetic structuring of contemporary samples in this study (Fig. 1c) and elsewhere (Quinn et al. 2022).

Heterozygosity

Estimates of autosomal heterozygosity indicated high variation for western montane red foxes (1.4 to 2.4 heterozygous sites per kb), spanning the range of heterozygosity observed in the east but significantly lower than either Alaskan or Eurasian representatives (2.8 and 3.2 heterozygous sites per kb, respectively; supplementary table S7, Supplementary Material online; Fig. 3a). The dispersion in estimates was principally caused by many windows

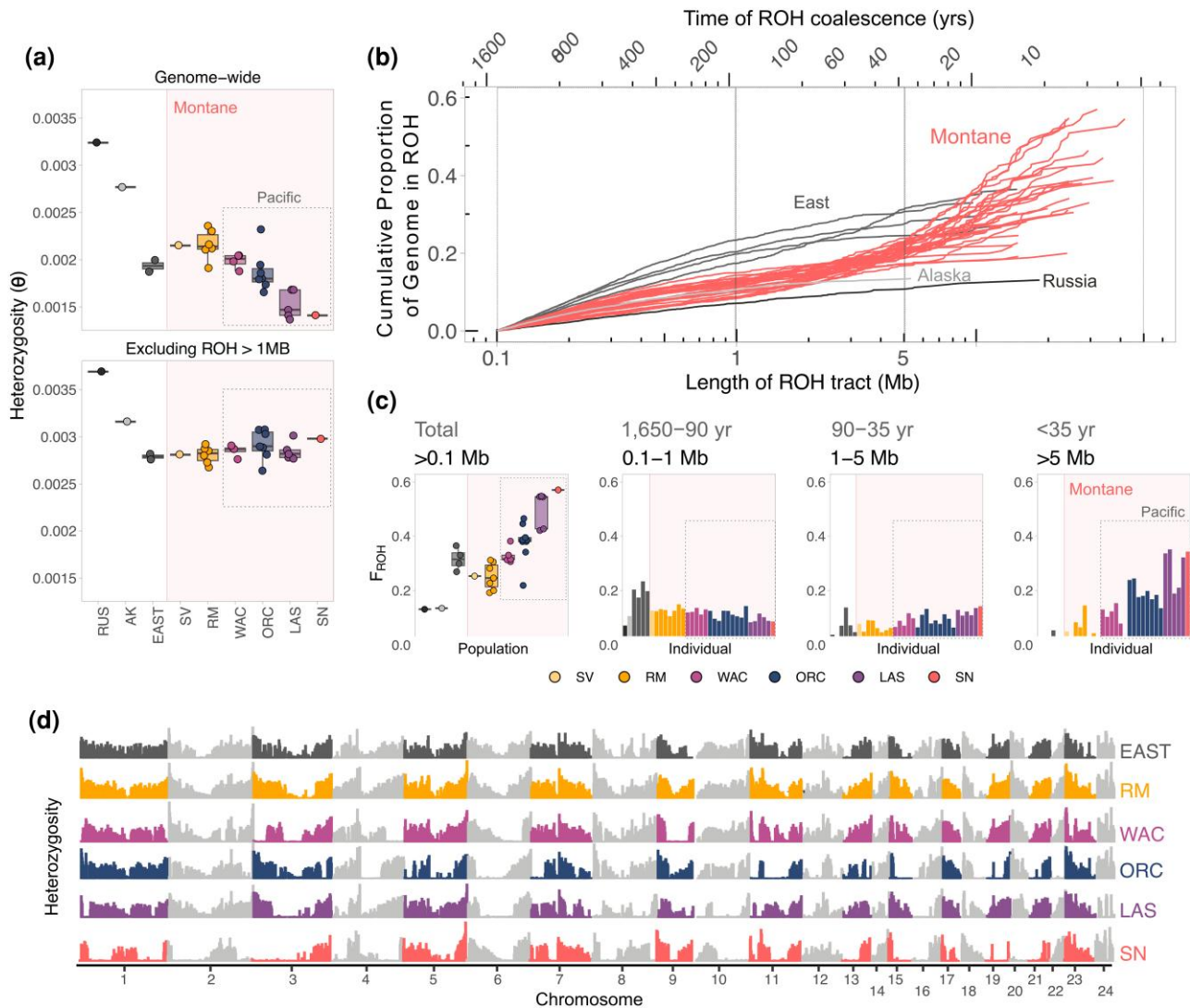


Fig. 3. Inbreeding and diversity. a) Estimates of heterozygosity genome-wide and after excluding ROH > 1 Mb in length. b) Cumulative proportion of the genome in ROH shorter than the length displayed on the x axis for 34 individuals. c) Contribution of different length classes of ROH to individual inbreeding coefficient. d) Genome-wide heterozygosity estimated over nonoverlapping 1-Mb for six representative individuals.

with no variation (i.e. ROH) in the Pacific mountain populations (Fig. 3b to d). When excluding ROH > 1 Mb, the heterozygosity mode was roughly equivalent across all montane populations, as well compared to the east (supplementary fig. S10, Supplementary Material online). Even the samples with the lowest genome-wide variation (SN and LAS) showed high autosomal heterozygosity values relative to other published values for carnivores. For comparison, African leopards (*Panthera pardus pardus*), leopard cats (*Prionailurus bengalensis*), banded mongoose (*Mungos mungo*), and honey badgers (*Mellivora capensis*) are other widely distributed species of Least Concern and have genome-wide estimates of ~ 2 heterozygous sites per kb (Pečnerová et al. 2021; Wilder et al. 2023). This “saw-tooth” pattern of high genomic variation interrupted by long invariable stretches (Fig. 3d) is more consistent with postcolonial declines than a long-term restricted N_e for Pacific mountain populations.

Inbreeding

We characterized the consequence of declining effective population size by quantifying ROH, or identical segments of the genome inherited from a common ancestor (Ceballos et al. 2018). Somewhat surprisingly, all sampled red foxes, even those from Russia and Alaska had a non-negligible portion (>13%) of their genome in ROH > 100 kb (supplementary table S7, Fig. 3c and e, supplementary fig. S10, Supplementary Material online). However, by far the highest levels of inbreeding were found in the Pacific mountains, particularly in the SN ($F_{ROH > 100 \text{ KB}} = 0.57$) and LAS ($F_{ROH > 100 \text{ KB}} = 0.42$ to 0.55). These inbreeding coefficients approached estimates from some of the most iconic examples of inbreeding in carnivores, such as Isle Royale wolves (Robinson et al. 2019), Florida panther (*Puma concolor*) (Saremi et al. 2019), and Indian tigers (*Panthera tigris*) (Khan et al. 2021). Although eastern red foxes also had moderate levels of autozygosity ($F_{ROH > 100$

$k_B = 0.27$ to 0.37), they differed from montane populations in their length profiles (Fig. 3c and d, supplementary figs. S10 and S11, Supplementary Material online). Most ROH in eastern foxes were <1 Mb, consistent with rapid growth from the bottleneck inferred by GONE. The montane group also had substantial ROH <1 Mb, but most ROH were longer tracts that coalesced in the last century. Within the montane group, the Pacific mountain populations had more long ROH than RM red foxes, with Lassen and SN individuals showing 8%–25% of their genome in ROH >10 Mb. Pairwise comparisons indicated high sharing of ROH haplotypes within montane populations and low sharing among populations, confirming most inbreeding happened after montane populations became isolated from each other (supplementary fig. S12, Supplementary Material online).

Deleterious Variation

We used SnpEff (Cingolani et al. 2012) to identify 111,860 variable sites in 27,192 protein-coding genes: 69,025 synonymous, 42,124 missense, and 711 loss-of-function (LoF) variants. Of the missense variants, we discarded the 63% that were predicted by SIFT (Vaser et al. 2016) to be tolerated and only retained the 15,770 sites predicted to cause an amino substitution deleterious to protein function. Missense and LoF derived variants had lower average frequencies relative to intergenic and synonymous derived variants (supplementary fig. S13a, Supplementary Material online), validating that SnpEff and SIFT could discern deleterious from benign protein change.

Frequencies of putatively deleterious missense and LoF alleles were higher in the montane group compared to the east (supplementary fig. S13b, Supplementary Material online), but similar across montane populations. Within the montane lineage, genotypic distribution of deleterious variants appeared to be strongly influenced by recent declines. Populations with the most severe reductions in the Pacific mountains (i.e. high $F_{ROH > 1 \text{ Mb}}$) had fewer sites with deleterious alleles (potential load; Fig. 4a) but many more deleterious alleles in homozygous form (realized load; Fig. 4b). Moreover, both indices were highly correlated with $F_{ROH > 1 \text{ Mb}}$, indicating these patterns were associated with recent inbreeding. On average, an increase of $F_{ROH > 1 \text{ Mb}}$ from 0.1 to 0.5 translated to a reduction in the number of sites with potential to contribute a deleterious allele by 10% to 20%, and a rise in the number of sites with homozygous deleterious alleles $\sim 25\%$ to 30%. The relationships between recent genomic inbreeding and realized load were weaker for LoF than missense mutations, possibly due to lower statistical power (only 711 sites compared to 15,770, respectively) or the influence of purifying selection (i.e. purging).

To investigate the role of selection directly, we calculated the total number of putatively deleterious alleles, which should be equivalent among populations when drift is the dominant evolutionary forces (Kirkpatrick and Jarne 2000). For missense alleles (i.e. small-effect), we observed

a weak positive linear relationship with $F_{ROH > 1 \text{ Mb}}$, in which an increase in $F_{ROH > 1 \text{ Mb}}$ from 0.1 to 0.5 predicted 3% more deleterious alleles in the inbred populations (Fig. 4c). This suggests selection has been less influential at reducing numbers of small-effect deleterious alleles in inbred relative to more outbred populations. In contrast, we observed no linear relationship between the total load of LoF deleterious alleles (i.e. large-effect) and $F_{ROH > 1 \text{ Mb}}$ (linear $R^2 = 0.0$, $P = 0.30$). Instead, the pattern suggested a quadratic relationship between LoF allelic load and inbreeding (quadratic $R^2 = 0.28$, $P = 0.01$). This could reflect a “goldilocks” phenomenon for purging, whereby inbreeding is positively associated with removal of recessive deleterious alleles up to a point, beyond which, selection against deleterious alleles becomes overwhelmed by drift, resulting in reduced purging. Correspondingly, although numbers of sites with at least one deleterious allele decreased monotonically with elevated inbreeding (Fig. 4a), the California populations (SN and LAS) that suffered the most severe declines had 20% to 40% more homozygous missense and LoF deleterious alleles than did the more robust RM population (Fig. 4b). In contrast, the ORC and WAC populations, with more moderate declines, had similar numbers of homozygous LoF alleles to that of the RM population, despite their higher inbreeding.

Compared to the RM population, which most closely represented ancestral levels of variation, LAS and ORC had “L-shaped” site-frequency spectra, consistent with their small sizes (Fig. 5a). The LAS population in particular had a strong second mode corresponding to fixed derived alleles, which applied to deleterious as well as putatively neutral alleles, as expected from drift in a small population. As a result, these Pacific mountain populations had fewer sites with deleterious alleles overall but higher frequency of deleterious alleles at remaining sites (Fig. 5b). For example, LAS had approximately two-thirds of the deleterious variants present in RM but three times as many fixed deleterious alleles. Fixed deleterious variation is particularly relevant to conservation planning because it represents a loss of fitness that can only be reversed through future gene flow. Finally, we used R_{XY} (Do et al. 2014; Xue et al. 2015) to compare the frequency of derived alleles shared between populations. An R_{XY} equal to one corresponds to no change in allele frequencies and an R_{XY} greater or less than one corresponds to an increase or decrease in frequency of alleles in population X relative to population Y, respectively. Both LAS and ORC experienced a negligible accumulation of missense-deleterious alleles but a more substantial deficit of LoF alleles compared to RM, although 95% confidence intervals overlapped one for all but the moderate-sized ORC population (Fig. 5c). Interestingly, montane populations had similar or higher accumulation of deleterious alleles than the eastern group, suggesting negligible long-term purging compared to other North American red foxes as well (supplementary fig. S14, Supplementary Material online). Together population-based analyses for the montane lineage suggest drift and inbreeding during anthropogenic declines have rearranged

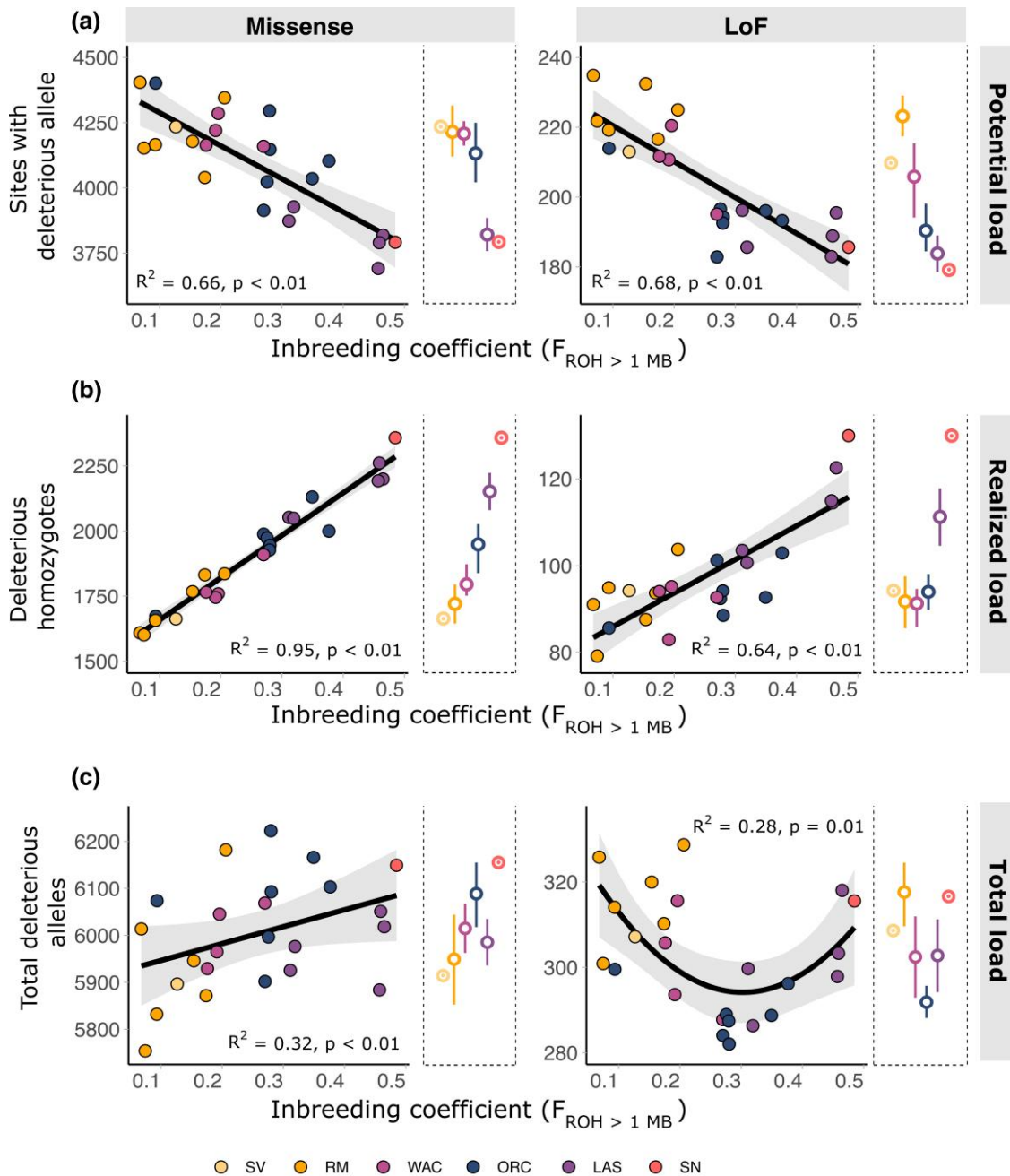


Fig. 4. Individual-level genetic load of western subpopulations. Relationships of recent inbreeding to proxies of genetic load: a) number of sites with at least one deleterious allele, b) number of sites with deleterious, homozygous alleles, and c) total number of deleterious alleles. Open circles in the right panel show the mean estimate of load for each western subpopulation and the error bars represent 95% bootstrap confidence intervals; populations represented by a single sample are denoted with a dot. Estimates were based on 15,770 missense and 711 LoF mutations.

the potential load into realized homozygous load, with purifying selection playing a lesser role, significantly influencing only LoF mutations in the moderate-sized ORC population.

To investigate how the distribution of deleterious variation across populations might influence selection of source populations for the purpose of genetic rescue, we focused a set of analyses on the Lassen population (LAS) as the recipient of genetic augmentation (Fig. 6, supplementary fig. S15, Supplementary Material online).

We compared deleterious allelic contributions from two candidate donor populations: ORC, moderately inbred and connected within the last century, and RM, most diverse but isolated from LAS a thousand years longer. As expected, both candidate donor populations shared similar numbers of homozygous derived alleles with LAS, suggesting they would be equally effective at masking deleterious alleles in the recipient population (Fig. 6a, supplementary fig. S15a and d, Supplementary Material online). However, as there is potential for donor

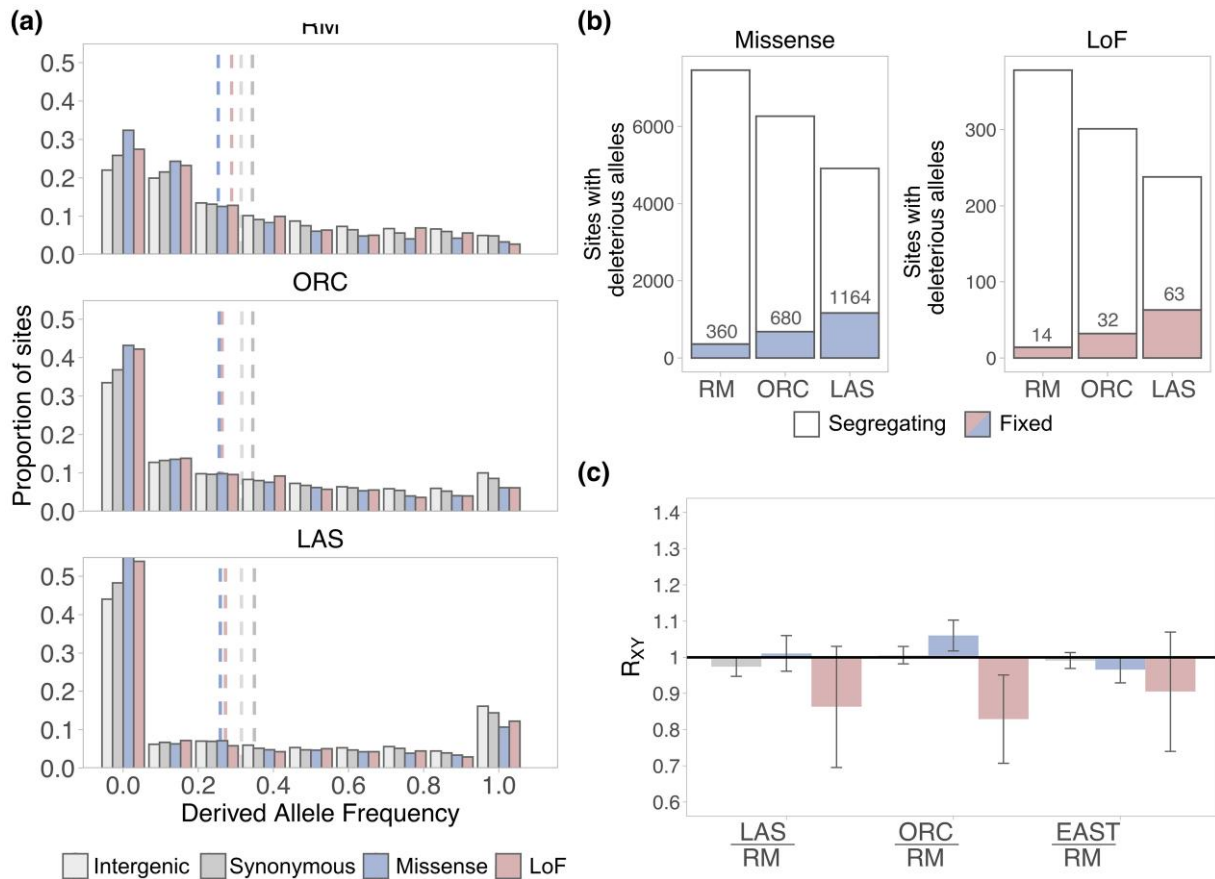


Fig. 5. Population-level genetic load of western populations. a) Derived SFS for three western populations, including fixed (frequency = 1.0) and missing (frequency = 0) alleles. Dashed lines show the average allele frequency for each mutational class. b) The number of sites with putatively deleterious alleles that are segregating and fixed for each population. c) Frequency of derived mutations in population X relative to population Y (R_{XY}). Error bars indicate $2 \pm SE$.

individuals to breed with each other (or their progeny) in the augmented population, we also considered the number of homozygous genotypes shared within donor pairs. Here, two donor haplotypes masked fewer deleterious alleles in each other when they originated from ORC than from RM (Fig. 6b, supplementary fig. S15b and e, Supplementary Material online). However, ORC donors also had significantly fewer LoF alleles not found in the recipient gene pool (Fig. 6c, supplementary fig. S15c and f, Supplementary Material online). Using ORC as a donor population therefore would likely introduce fewer LoF variants overall, but more of them in homozygous form, compared to the larger, more diverse RM population.

Discussion

We used whole genome sequences to advance ongoing conservation planning for western montane red foxes in North America. By contextualizing their current scarcity in terms of their historical and ancient past, our findings help guide recommendations regarding the suitability, priority, and implementation strategy for genetic rescue. First, our data support the hypothesis that the most prominent divisions among native montane red fox populations are

evolutionarily young, evolving only in the latter half of the Holocene. Second, despite a shared long-term history, the regional differences in the genetic status of contemporary montane populations are stark. Historical fragmentation and isolation have reduced N_e to concerning levels in all four remnant Pacific mountain populations, particularly the southernmost two in California. Comparatively, representatives from the northwestern Rocky Mountains have retained more ancestral diversity. Finally, our results suggest that although purging may have lessened the severity of inbreeding depression in some populations, its benefits may be slight compared to the loss of fitness from increased homozygosity due to drift and inbreeding. Together, these findings suggest a severely fragmented metapopulation that could benefit from translocations to promote genomic restoration. However, while genetic rescue has the potential to improve viability generally, outcomes for the smallest populations may be particularly sensitive to the deleterious burden carried by donor individuals.

Large Long-term Effective Size and Recent Anthropogenic Declines

Our analyses of genomic sequences were in agreement with the fossil record in indicating that red foxes have

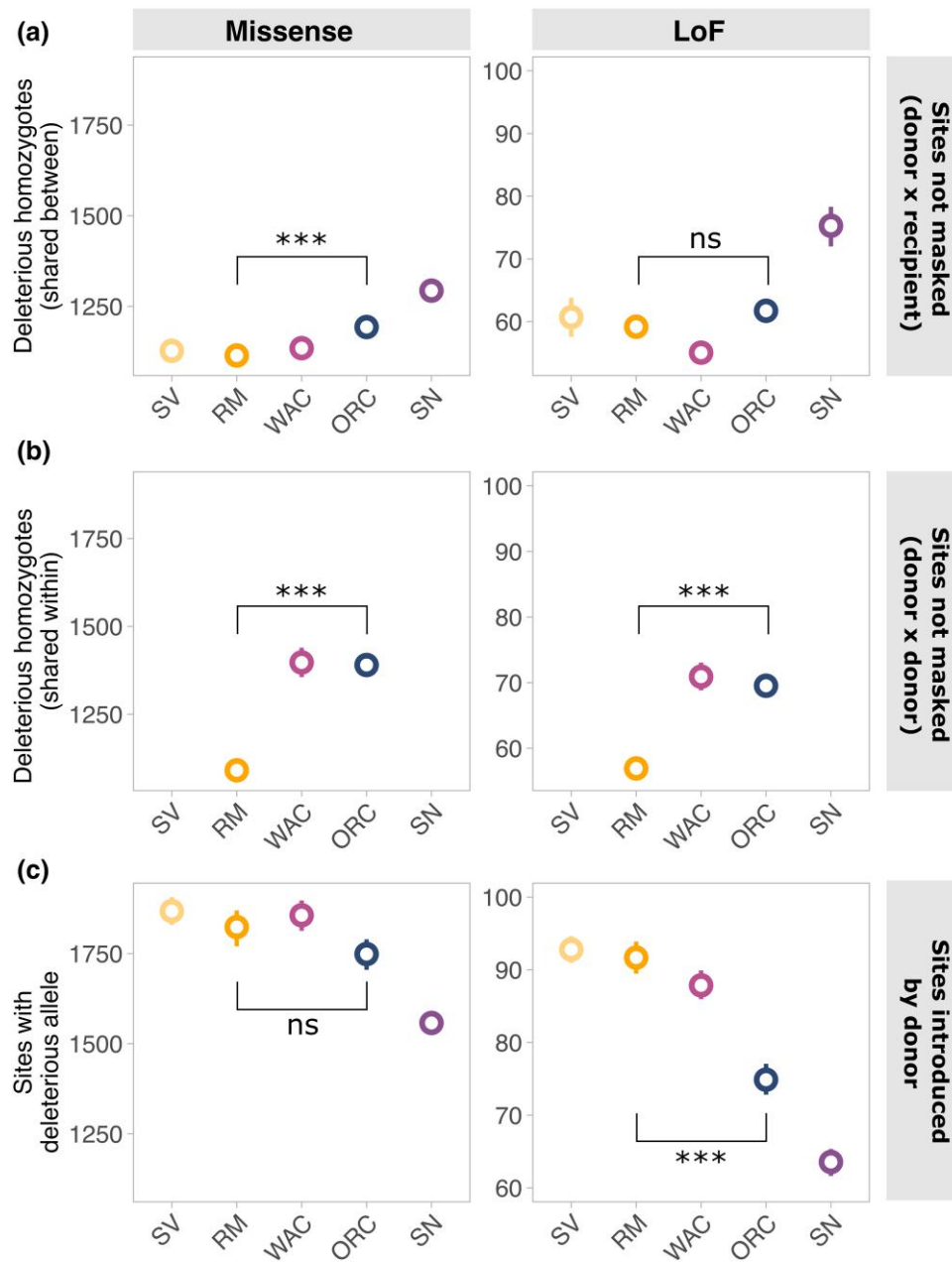


Fig. 6. Comparison of load between candidate donor populations and the LAS population as the intended recipient. The average value of load metrics calculated between pairs of individuals in two populations. a) The number of sites where both the donor and recipient individual are homozygous for the same derived allele, representing the failure to mask recessive deleterious alleles in progeny. b) The number of sites where two donor individuals are homozygous for the same derived allele, representing the potential for load to be expressed in later generation progeny. c) The number of sites where the donor individual has a derived allele and the recipient individual does not, representing the potential for introduction of deleterious alleles at new sites in progeny. Open circles show the mean value over every pairwise comparison and the error bars represent 95% bootstrap confidence intervals. Significance levels for ORC and RM comparison: ns, not significant at $\alpha = 0.05$; *** $P < 0.001$.

been abundant in North America since their initial migration over the Bering land bridge approximately 300,000 years ago (Péwé and Hopkins 1967). Founders of the North American lineage originated in Siberia and were, therefore, likely preadapted to the cold climate and open vegetation structure of glaciated North America. Even after sequestration in isolated refugia south of the ice sheets, our reconstructions of N_e and climatic niche suggest that montane red foxes remained abundant, widespread, and genetically diverse. Our sequential Markovian

coalescent reconstructions indicated gradual declines in N_e only after glaciers began retreating (Fig. 4a and b). During this time, climate models predicted a coinciding contraction of the thermal niche: boreal conditions became increasingly fragmented and restricted to the footprint of the western cordilleras until climate stabilized mid-Holocene (Fig. 4f). Montane subspecies likely differentiated during this upward retreat of boreal-like habitat into the mountains (Aubry et al. 2009). While MSMC2 and climate reconstruction indicated its establishment around

6,000 years ago, ABC modeling predicted more recent divisions, ~1,000 to 3,000 years in the past. Other lines of evidence supporting the long-term shared ancestry of montane red foxes include high heterozygosity outside of ROH, short internal branches in the neighbor-joining tree, and the near-complete absence of fixed mutational differences (supplementary table S8, Supplementary Material online). Subspecific designations appear to better capture early differentiation of a once-continuous, geographically structured metapopulation, rather than deeply divergent lineages.

Genomic findings instead highlight contrasts in recent demographic trajectories of montane populations. Low genetic diversity of Pacific mountain populations seems to primarily be a consequence of historical declines and isolation. Both ROH and LD-reconstructions of N_e indicate steep population declines beginning in the 1800s, coinciding with westward expansion of the North American fur trade following the Lewis and Clark expedition in 1,805 (Obbard et al. 1987). Interestingly, both ROH and LD detected signatures of bottlenecks in eastern red foxes as well, suggesting the impacts of market trapping may have been range-wide, similar to fisher (*Pekania pennanti*), beaver (*Castor canadensis*), and other lucrative furbearers (Tapper and Reynolds 1996). If so, it is not obvious why declines would be transient in eastern Canada and the Rocky Mountains but persistent in Pacific mountain populations, where inbreeding has continued into recent decades.

The disparity in resilience may be partly attributable to the distinct configurations of upper montane habitat in the western United States. Simulations have shown that local extirpations result in higher inbreeding rates among surviving populations in stepping-stone metapopulations, as likely the case in the linear Cascade and Sierra Nevada ranges, than in island models, which may more closely resemble the clustered ranges of the northern Rocky Mountains (Kurland et al. 2023). Our ABC modeling tentatively supports this hypothesis, showing that isolation of the Lassen population coincided with extirpation of the nearby Shasta population—a probable stepping-stone that facilitated gene flow with Oregon Cascade red foxes (Grinnell et al. 1937). Given the overall shallow levels of genetic differentiation, it seems plausible that human driven declines disrupted low-level or intermittent gene flow between more geographically (and genetically) distant populations as well. Although we did not have the widespread sampling to test directly, museum samples dated to a century ago also indicated lower genetic distances and higher haplotype sharing than at present, consistent with greater past connectivity (Aubry et al. 2009; Sacks et al. 2010; Volkmann et al. 2015). Regardless, historical fragmentation of the Sierra Nevada subspecies illustrates how anthropogenic stressors and landscape configuration can synergistically act to rapidly elevate inbreeding—a consideration especially relevant for montane species in the context of climate change.

Suitability of Genetic Rescue as a Management Tool

A large long-term N_e and high heterozygosity maintained by gene flow throughout most of the Holocene suggest tradeoffs in the viability of contemporary montane red fox populations. On one hand, commensurate with high genome-wide diversity are many low-frequency, highly deleterious recessive alleles. This potential load of deleterious variation, or inbreeding load, stays hidden in heterozygous form when N_e is high, but serves as fuel for inbreeding depression when population density decreases. Because the inbreeding load is predominantly created by accumulation of novel mutations over tens or hundreds of millennia (van der Valk et al. 2021; Wootton et al. 2023), it may be that red foxes are especially predisposed to severe inbreeding depression following human persecution or over-exploitation (Hedrick and Garcia-Dorado 2016; Kardos et al. 2021; Bertorelle et al. 2022). Similar to gray wolves, mountain lions, arctic foxes, and other widespread generalists (Liberg et al. 2005; Norén et al. 2016; Saremi et al. 2019), the current scarcity of Pacific mountain red foxes could be in part propelled by their past success.

On the other hand, the recency of declines optimistically predicts that genomic restoration of montane red foxes is possible. The montane group has retained considerable standing genetic diversity outside of long ROH, suggesting the broader metapopulation has also retained high adaptive potential to future environmental change (Ørsted et al. 2019). Risk of outbreeding depression within the montane group is also predicted to be low. Whereas translocations within montane subspecies would restore historical connectivity, movement between montane subspecies could connect populations isolated before the postcolonial baseline, but likely not longer than a few millennia. Frankham et al. (2011) recommend <500 years of isolation to confidently avert outbreeding depression. However, this threshold is considered extremely conservative. Significant adaptive differentiation between wide-ranging mammals is likely to require many thousands of generations to evolve, especially for populations inhabiting similar environments (Frankham et al. 2011). For context, Florida panthers were augmented with individuals from a population in Texas estimated to have diverged 7,000 to 8,000 years earlier (Blischak et al. 2020); five generations later, no outbreeding depression was evident (Onorato et al. 2024). Our genome-wide analyses thus did not reveal a compelling reason to exclude translocations between montane subspecies on the basis of outbreeding depression, especially in lieu of alternatives.

There are several caveats to our findings, most notably that our analyses were based on limited sampling. Within Pacific mountain populations, samples were unavoidably inbred and closely related, which can bias demographic inferences (Blischak et al. 2020; Mather et al. 2020; Waples 2024). In turn, Rocky Mountain samples were collected over a wider geographic scope, but still a narrow representation of a vast and heterogeneous metapopulation. Our study certainly did not capture the full breadth of genetic and

demographic variation that comprises the Rocky Mountain subspecies. For example, previous studies have demonstrated the Rocky Mountain region contains pockets of non-montane ancestry introgressed from fur farms and possibly natural expansion of other refugial lineages (Quinn et al. 2022). One sample from Nevada in the present study indeed reflected discernable amounts of eastern ancestry. Although we excluded this individual from demographic analyses, we did not explicitly account for the possibility of eastern gene flow in our demographic models, which could both distort site frequency analyses and elevate risk of outbreeding depression. In theory, selective introgression of only a few genes is potentially sufficient to alter montane red foxes from their historical phenotype. Limited morphological data suggest this is a possibility, with larger body size reported in some contemporary northern Rocky Mountain populations than indicated by museum specimens (see Quinn et al. 2022). To address remaining concerns of outbreeding depression, the most expedient approach may be to conduct localized ecological studies that confirm ecological, morphological, and phenological overlap (e.g. seasonal onset of estrus) between recipient and source populations.

Consequences of Historical Declines on Deleterious Load

Understanding how demographic history shapes the distribution of deleterious variation has become a prominent issue in conservation biology (Bertorelle et al. 2022; van Oosterhout et al. 2022; Dussex et al. 2023; Robinson et al. 2023). From genomic studies of demographic bottlenecks that lasted hundreds to thousands of generations, a consensus is emerging that small N_e simultaneously results in purging of strongly deleterious alleles and accumulation of weakly to moderately deleterious alleles (Xue et al. 2015; Robinson et al. 2018; Dussex et al. 2021; Mathur and DeWoody 2021; Kleinman-Ruiz et al. 2022). The implications are that ancient bottlenecks insulate populations from the most severe and immediate fitness consequences of declines caused by anthropogenic activities, possibly explaining why some highly inbred populations do not show obvious phenotypic signs of inbreeding depression. We did not observe strong evidence of long-term purging in montane red foxes relative to other lineages. Despite a smaller contemporary N_e than eastern red foxes, R_{XY} analyses indicated that montane populations carried a similar or greater burden of deleterious alleles relative to their eastern counterparts, presumably due to a larger refugial N_e during the last glaciation.

The efficacy of purging to mitigate inbreeding depression over anthropogenic time scales is more equivocal (Hedrick and Garcia-Dorado 2016). We observed evidence of purging of LoF alleles only in populations subject to less severe declines in the northern Pacific mountains. In contrast, the California populations, which underwent the most severe and rapid declines, showed weaker evidence of purging. The influence of purging on such recent time-scales similarly varies across studies, ranging from no

evidence of purging at all (Robinson et al. 2019; Ochoa et al. 2022; Smeds and Ellegren 2023), purging in the most deleterious class of mutations only (Grossen et al. 2020; Khan et al. 2021), and accumulation across all classes of deleterious mutations (van der Valk et al. 2019). It is challenging to discern the degree to which these idiosyncrasies are due to methodological choices, statistical power, quality of the annotation, or true evolutionary processes. Our results supported a dominant role of drift and inbreeding in shaping the genetic load, with the expected tradeoff between higher potential load in larger populations and higher realized load in smaller populations (Bertorelle et al. 2022; Dussex et al. 2023). At a more nuanced level, our findings lend support to the notion that the efficacy of purifying selection is sensitive to the rate of decline and inbreeding (Hedrick and Garcia-Dorado 2016). This pattern of more efficient purging in moderately inbred populations is consistent with previous studies showing long ROH are enriched for deleterious variation relative to shorter, older ROH (Szpiech et al. 2013; Stoffel et al. 2021), and, unsurprisingly, predicts the greatest risk of inbreeding depression for the most drastically reduced populations.

Conservation Implications

Our findings suggest inbreeding depression may be significantly impacting viability of the Lassen and Sierra Nevada populations in California. Monitoring data suggest an unmanaged genetic rescue is already underway in the Sierra Nevada (Quinn et al. 2019), making Lassen the higher priority for intervention. The Sierra Nevada population was represented in this study by a single genome collected in 2011, prior to the start of low-level immigration from a neighboring population in the Great Basin. Immigration was immediately followed by admixture, increased reproductive output, and an expanding distribution of admixed progeny (Quinn et al. 2019; Hatfield et al. 2021). The apparent heterosis supports substantial inbreeding depression in the Sierra Nevada population, and by extension, presumably the Lassen population as well. Whereas monitoring efforts have demonstrated that low-level gene flow continues to bolster the Sierra Nevada population (unpublished data), the Lassen population remains isolated with a single migrant detected in over 20 years of monitoring (Quinn et al. 2022; Sierra Nevada Red Fox Conservation Advisory Team 2022). Telemetry studies in Lassen have further confirmed few breeding pairs and small, infrequent litters (Sierra Nevada Red Fox Conservation Advisory Team 2022), which, along with genomic estimates of elevated ROH and homozygous deleterious alleles, implicate inbreeding depression as a proximate factor limiting growth of the Lassen population.

However, the characteristics of the Lassen population that makes the case for genetic rescue so compelling also make its success highly uncertain. With an estimated abundance fewer than 30 individuals (Sierra Nevada Red Fox Conservation Advisory Team 2022; Green et al. 2023), the persistence of the Lassen population is

precarious. Any factor that increases variance in fitness, even transient, could tip the population toward extirpation. So although genetic rescue may ultimately reduce both inbreeding and genetic load and raise mean fitness, in the short-term it imposes a period of high stochasticity that could elevate extinction risk (Pérez-Pereira et al. 2022). In an ideal genetic rescue, an infusion of novel variation would reduce the expression of recessive alleles, improve fitness enough to spur rapid population growth, and permanently convert the realized load to its ancestral masked form. More realistically, such growth is likely to ensue over generations for carnivores with low fecundity and long lifespans, such as montane red foxes (Quinn et al. 2019). During this gradual growth phase, the Lassen population could stay small enough that continued inbreeding would be unavoidable. This “recovery bottleneck” would create an opportunity for the donor load to recombine in homozygous form and impose a fitness cost that is additional to the current inbreeding depression. The greater the current inbreeding depression, the more probable this scenario, as higher-fitness progeny of donor stock will disproportionately contribute their genetic material to subsequent generations (Harris et al. 2019).

The ideal source population for genetic rescue of small populations would thus balance the need to reverse current inbreeding depression with the need to counter future inbreeding depression caused by potential load in the donor population. Currently, managers are considering genetic rescue of the Lassen populations using two candidate donor populations, both sourced from Oregon: the larger, genetically diverse Rocky Mountain red fox population occupying the Blue Mountains ecoregion and the more moderate-sized Cascade population that belongs to the same (Sierra Nevada) subspecies but also has higher inbreeding. Because inbreeding in Lassen occurred after its isolation, donors from both populations are expected to be equally effective at masking the realized load in Lassen. However, the differences in potential and realized load between donor populations create tradeoffs between the severity of fitness consequences and the rate of return for inbreeding. Based on pairwise comparisons, translocated red foxes from the Oregon Cascades would on average introduce fewer sites with novel deleterious alleles than foxes in the Oregon Cascades red foxes, especially for the highly deleterious LoF category, which would minimize the severity of additional inbreeding depression that could occur during a recovery bottleneck. However, more of the deleterious alleles introduced would be embedded in ROH segregating at high frequencies in the donor population and would thus be more likely to be shared with other translocated individuals. This higher frequency within the donor population could hasten the return of inbreeding and increase the probability that it involves donor haplotypes.

Currently, no clear decision framework exists to navigate this tradeoff between the rate of return of inbreeding and its potential severity. The influence of deleterious variation on translocation success is primarily supported by theory and simulations (Hedrick and Garcia-Dorado 2016; Kyriazis

et al. 2021; Pérez-Pereira et al. 2022), with limited empirical evidence (Hedrick et al. 2019; Wilder et al. 2020). Consequently, many conservation geneticists caution against prioritizing putatively functional variation in management decisions, which could result in unintended, adverse effects (Ralls et al. 2020; Kardos et al. 2021). Pragmatically, the choice of donor population is likely to be dictated by nongenetic factors, such as phenotypic similarity, administrative logistics, and most critically, the abundance of the donor population and its ability to sustain removals. Given the inherent complexity of rescuing extremely small populations, a plan to monitor postaugmentation and adaptively manage for sustained growth or periodic connectivity may prove more important in the long-term.

Our results show varying degrees of localized inbreeding of a formerly large and genetically diverse metapopulation. This finding is hopeful for the conservation prospects of montane red foxes, as it broadens the range of possibilities for restoring diversity to genetically depleted populations in the Pacific mountains. Promoting robust populations may serve conservation of these small, isolated populations more than endeavors to preserve unique genetic diversity that is largely drift-driven. However, our findings also present a challenge to long-term management planning, as they suggest montane red foxes will not be fully recovered until metapopulation dynamics are restored across the western United States. Ensuring enough migration to prevent accumulation of inbreeding in the Pacific Mountains will likely require either increases in size of, or the creation of new populations to serve as stepping stones. These goals are not easily achieved and will require sustained, multistate efforts. Genetic rescue may serve as a short-term tool to accomplish these goals but alone are unlikely to be a sufficient solution.

Methods

Samples and Sequencing

We extracted genomic DNA from either tissue or blood of 34 red foxes that were collected from lived-trapped animals for other studies (whose methods followed American Society of Mammalogists animal care guidelines; Sikes and Bryan 2016), road strike mortalities, or skins from licensed fur trappers (Fig. 1a, supplementary table S1, Supplementary Material online). Of these, 28 originated from the montane lineage of the western U.S. We included samples from three discrete and isolated populations of the Sierra Nevada subspecies (*V. v. necator*; ORC, SN, LAS) and one from the Cascade subspecies (*V. v. cascadenis*, WAC), which we collectively refer to as the Pacific mountains. To represent the Rocky Mountain subspecies (*V. v. macroura*), we sequenced samples from eastern Oregon and Nevada (RM), which are of mainly native Rocky Mountain subspecies ancestry despite overlap with Great Basin and Columbia Plateau ecoregions (Quinn et al. 2022). For complete representation of the montane lineage, we also included an individual from the Sacramento Valley (SV), which represents a phenotypically and ecologically distinct subspecies (*V. v. patwin*)

endemic to the low-elevation, arid Central Valley region of California (Sacks et al. 2010). Finally, to contextualize genetic comparisons among montane populations, we sequenced samples from the eastern refugial lineage (Newfoundland = 3, Vermont = 1), from Alaska to represent the third northern refugial lineage in North America ($n = 1$), and from Yamal, Russia ($n = 1$) as an outgroup to all North American red foxes (supplementary table S1, Supplementary Material online).

DNA was extracted using the Qiagen DNEasy Blood and Tissue Kit (Qiagen Inc, Valencia, CA) following manufacturer's instructions. To generate whole genome shotgun sequences, we constructed indexed libraries using NEBNext® Ultra™ DNA Library Prep Kit for Illumina® according to manufacturer's instructions but scaled to half-reaction volumes, along with custom Illumina-compatible indexes. Libraries were then cleaned and size selected using Agencourt AMPure XP beads (Beckman Coulter), quantitated using a Qubit 2.0 dsDNA BR fluorometer, and submitted for 150-bp paired-end sequencing on Illumina HiSeq 4000 or Novaseq 6000 lanes at the UC Davis Genome Center and Admera Health (South Plainfield, NJ).

Bioinformatics

We used Trim-galore (Krueger 2012), a Perl wrapper around the Cutadapt v.1.8.3 (Martin 2011) and FastQC v.0.11.9 (<https://www.bioinformatics.babraham.ac.uk/projects/fastqc>), to trim adapters from raw reads and discard sequences <30 bp. We aligned reads to an arctic fox reference genome (Peng et al. 2021) using the mem algorithm of the Burrows-Wheeler Aligner (BWA) v.0.7.17 (Li 2013). We also mapped a subset of samples to the red fox (v.2.4; Rando et al. 2018) and domestic dog (CanFam3.1) references and identified the arctic fox as offering the best compromise between minimizing phylogenetic divergence and maximizing assembly and annotation quality (supplementary fig. S16, Supplementary Material online). We used Samtools v.1.16 (Li et al. 2009) to sort and remove secondary alignments and read pairs where only a single read mapped. We marked duplicates, added read groups, and collected basic alignment statistics with Picard v2.7.1 (<https://broadinstitute.github.io/picard/>) and used Genome Analysis ToolKit (GATK) v.3.8.1 (<https://software.broadinstitute.org/gatk/>) to conduct local realignments around indels. The filtered reads resulted in depths of genome coverage that ranged from 5 to 51× with 80% of samples >10×.

To avoid assumptions of Hardy–Weinberg equilibrium, we called variants separately for each individual using bcftools (v.1.16; <https://samtools.github.io/bcftools/>) mpileup and bcftools call (option “–group-samples–”). We required minimum mapping and base qualities >30 and excluded sites with >2 or <1/3 the mean pooled depth (576×). We used bcftools to retain only biallelic SNPs with at least five reads supporting the minor allele (“INFO/AD[1] > 5 && INFO/AD[0] > 5”), a site quality phred score >100 (“%QUAL≥100”), a minimum of 5 bp distance from indels (“-g 5”), and, to exclude paralogs,

fewer than 80% of individuals with heterozygous genotypes (“F_PASS(GT = “het”) ≥ 0.80”). To minimize genotyping error caused by contamination, misalignments, and sequencing errors, we required all genotypes to have at least three reads (-e “FMT/DP < 3”), heterozygous genotypes to have at least 20% of the total reads supporting the minor allele (-e “GT = “HET” & (sMin(FORMAT/AD)/FORMAT/DP) < 0.2 ”), and homozygous genotypes to have <20% of reads containing a second allele (“GT = “HOM” & (-e “sMin(FORMAT/AD)/FORMAT/DP) > 0.2”). We used bedtools2 v.2.3 (Quinlan and Hall 2010) to exclude unplaced scaffolds, the X chromosome, and regions of poor mappability that were identified using Genmap (Pockrandt et al. 2020) based on a k-mer length 100 and allowing for 2 mismatches. Finally, we excluded sites with >20% missing data, for a final dataset consisting of 16,707,287 biallelic variants.

Population Structure

To analyze population structure, we first pruned variants in strong LD using the LD pruning function (indep-pairwise 100 10 0.2) in Plink v1.9 (Purcell et al. 2007), resulting in 817,577 variants. We used Plink to conduct a principal component analysis (PCA) and to calculate a pairwise matrix of identity-by-state which we used to construct a neighbor-joining tree in R program ape (Popescu et al. 2012). We also used the program Admixture v1.3.0 (Alexander et al. 2009) to identify genetic clusters within our dataset. We ran Admixture 10 times each for clusters $K = 1$ to 15 and selected the runs with the highest likelihood for visualization of each K . We used cross-validation error to characterize the stability of cluster assignments. To adjust for unequal sample sizes and inbreeding, we then repeated PCA and Admixture analyses with a maximum of two samples per montane population, preferentially retaining unrelated individuals identified using the KING moment approach (Manichaikul et al. 2010) in Plink v2.0 (Chang et al. 2015).

Demographic Reconstruction

We used multisequentially Markovian coalescent (MSMC2; Schiffels and Wang 2020) to infer long-term effective population sizes through time and approximate divergence between populations. MSMC2 uses heterozygosity across genomic segments to estimate coalescent rates, which are inversely related to population size in the absence of substructure. When applied to a single genome, MSMC2 is equivalent to pairwise sequentially Markovian coalescent (Li and Durbin 2011) but with an algorithm that improves recombination estimates. MSMC2 also can incorporate phased haplotypes from multiple individuals to increase the number of coalescent events within a population and heighten resolution over more recent time periods. As we only had one sample from Russia and from Alaska, we first ran MSMC2 with a single representative genome (two haplotypes) from each refugial lineage in North America and the Eurasian outgroup to visualize overall patterns of N_e .

To focus on recent demographic events in the western mountains, we then additionally ran MSMC2 using the two highest-coverage samples (four haplotypes) for the eastern lineage and per population in the montane lineage (LAS, ORC, WAC, and RM). For all runs, we phased samples with Shapelt4 v4.2.2 (Delaneau et al. 2019) using default parameters. We used the tool “bamCaller.py” from the MSMC-tools package to exclude sites with minimum mapping and base qualities <30, read depths less than half and 2× the average depth, and regions of low mapping quality identified by Genmap. We tested several parametrizations of atomic intervals (-p), including “4 + 25*2 + 4 + 6” and “1*2 + 16*1 + 1*2,” all of which produced similarly shaped trajectories but some of which resulted in unrealistic spikes in N_e in the most recent time intervals. Because the Holocene was the period of main interest, we opted to show results from “-t 15 -r 5 -p 10*1 + 22*2 + 4 + 6,” the parameterization that maximized resolution in recent time. To characterize variance, we bootstrapped estimates with 20 replicates of 240 Gb artificial genomes composed of 5 Mb resampled blocks. We scaled outputs to real time using a generation time of 2 years (Statham et al. 2018) and a mutation rate of 4.5e-9 mutations per site per generation estimated for gray wolves (Koch et al. 2019). We approximated divergence time between population pairs by estimating the coalescent rate of haplotypes across populations, ignoring ambiguously phased sites (-skipAmbiguous). We then calculated the relative cross coalescent rate (rCCR) as the ratio of the cross-population to the mean within-population coalescent rate. Values closer to 1.0 indicate panmixia whereas values closer to zero imply strict isolation. We considered the divergence process to have occurred during the interval between 0.25 and 0.75, with a 0.5 as a heuristic point estimate, as it represents the time when coalescence is twice as likely to occur within as between populations.

We reconstructed recent temporal trends of effective population sizes using patterns of LD in GONE (Santiago et al. 2020). As recent admixture distorts LD structure (Novo et al. 2023), we conducted runs separately for each population, using only the three Newfoundland samples for the eastern group fox and excluding three samples from montane populations that assigned to more than one population in the Admixture analyses. For all runs we ran 20 replicates, used unphased data and default parameters, and assumed a recombination rate of 0.6 cM/Mb (Kukekova et al. 2007).

We used an ABC framework (Beaumont et al. 2002) to estimate isolation times for montane subpopulations. Due to sample sizes constraints, we restricted consideration to three populations from two recognized subspecies: ORC and LAS of *V. v. necator*, and the RM of *V. v. macroura*. We used two modeling approaches that varied in complexity (supplementary fig. S6, supplementary tables S2 through S4, and Supplementary Material online). First, we constructed simplified two-population models wherein an ancestral population splits at time T_{DIV} but gene flow continues until time T_{ISO} (supplementary fig. S6a to c, supplementary table S2, and Supplementary Material online).

To avoid confounding ancient divergence and recent bottlenecks, we restricted TDIV to within 10,000 years and incorporated historical declines. At time T_{BOT} (60 to 120 years ago), populations experienced an instantaneous size change based on contemporary N_e estimates. We bounded priors for bottlenecked population size using the interquartile range of N_e estimated by GONE over the most recent 100 years for each population: RM 1250 to 2600, ORC 350 to 650, LAS 30 to 60 (units in haploid individuals). In the second approach, we extended this framework to more realistic 3-population models that incorporated stepping-stone migration (supplementary fig. S6d and e, supplementary table S4, and Supplementary Material online). For these we fixed the bottleneck time at 60 years ago and compared two migration patterns: one in which RM isolation precedes subdivision within between ORC and LAS and another with continued inter-subspecies gene flow following the LAS-ORC split. We generated 100,000 coalescent simulations for two-population models and 50,000 simulations for the more computationally intensive three-population models.

For all ABC analyses, we compared the joint site frequency spectrum (SFS) obtained from simulations to the observed joint SFS for RM, ORC, and LAS. We selected individuals that showed no admixture in the Admixture analysis ($n = 6$ each for RM and ORC, $n = 5$ for LAS) and, to minimize the influence of selection, included only intergenic sites that were pruned for LD with bcftools using an r^2 threshold of 0.1. Singleton alleles were removed to minimize the influence of genotyping error. We calculated the joint SFS using easySFS (Gutenkunst et al. 2009), resulting in 6,000 to 8,000 SNPs per population pair (supplementary table S8, Supplementary Material online). We converted the joint SFS to four summary statistics for ABC analysis: the fraction of segregating SNPs private to each population, shared polymorphisms, and fixed differences. ABC analyses were conducted using the R package abc v1.0 (Csilléry et al. 2012). We evaluated model fits with the observed data using PCA visualizations and goodness-of-fit statistics calculated with the function “gfit” (supplementary figs. S17 and S18, Supplementary Material online). We approximated the posterior probability of each model using linear regression based on neural networks with a tolerance of 1% and pooled posteriors for models with similar support, based on a Bayes factor <3 (supplementary table S5, Supplementary Material online). To select approach for posterior estimation and predict error rates of posterior estimates, we conducted 100 iterations of leave-one-out cross-validation with the simulated summary statistics (supplementary fig. S9, Supplementary Material online). Cross-validation error indicated that nonlinear regression based on neural networks (Blum and François 2010) outperformed rejection sampling, with the highest accuracy predicted using a weight decay rate (λ) of 0.01 for regularization. Adopting this approach, we estimated the 95% highest posterior density (HPD) log transformation of parameters, retaining 1% of simulations closest to the observed summary statistics across all supported models (i.e. model averaging). Mutation rate and generation time were set as in MSMC2 and GONE analyses.

Climate Niche Models

To relate long-term reconstructions of N_e to climatic niche availability and connectivity in the past, we used museum records to construct a climatic niche model for montane red foxes. To train the model, we downloaded red fox occurrence records from the Arctos database (<https://arctos.database.museum>, accessed on July 2023) and the National Museum of Natural History (<https://collections.nmnh.si.edu/>, accessed on July 2023). We subset records to localities in the western states and with collection dates prior to 1950 (supplementary table S9, Supplementary Material online) to avoid biases caused by recent declines and to minimize inclusion of nonnative red foxes introduced from fur farming. We also excluded records from within the native Sacramento Valley red fox range due to their distinct climatic associations (Sacks et al. 2010). We then thinned the total records ($n = 161$) to a minimum distance of 25 km between records to reduce spatial bias ($n = 68$). The 19 bioclimatic variables for the contemporary period (1979 to 2013) were obtained from Chelsea-Climate (Karger et al. 2017). We constructed climatic niche models using the Maxent algorithm via the R package maxnet v0.1.4 (Phillips et al. 2017). We used ENMeval v2.0.4 (Kass et al. 2021) to test 12 models: linear (L), quadratic (Q), and linear-quadratic (LQ) feature classes combined with regularization multipliers of 0.5 to 2 and a 0.5 step value. The top model was selected using the Akaike information criterion corrected for small sample sizes (AICc) (Burnham and Anderson 2004). We then projected the model to the following past climate scenarios obtained from paleoclim (Brown et al. 2018): the mid-Holocene (8.326 to 4.2 ka; Fordham et al. 2017), Heinrich Stadial 1 (17.0 to 14.7 ka; Fordham et al. 2017), and the LGM (ca. 21 ka; Karger et al. 2017).

Genome-wide Heterozygosity

We estimated genome-wide autosomal heterozygosity using two methods. First, we used mlRho v 2.9 (Haubold et al. 2010) to estimate the population mutation rate (θ), which under the infinite sites model approximates heterozygosity. Second, we created individual VCFs that contained variant and invariant sites with bcftools mpileup/call and calculated the fraction of heterozygous over total callable sites in nonoverlapping 1-Mb windows. We estimated genome-wide heterozygosity as the mean value across windows after excluding those that had >20% missing data. For both approaches, we only included individuals with mean depths >9 \times and, to mitigate the effects of misalignment, removed sites with mapping and base qualities <30, depths <5 or >2 \times the mean, and regions of low mappability identified with Genmap.

Runs of Homozygosity

Inbreeding can be quantified through ROH, which consist of long tracts of identical haplotypes inherited through a common ancestor (Kardos et al. 2016; Ceballos et al. 2018). We identified ROH using a hidden Markov model implemented with Bcftools/ROH v.1.16 (Narasimhan et al. 2016). We

calculated the cumulative fraction of the genome in ROH (F_{ROH}) by summing all ROH >100 Kb and dividing by the length of the callable genome (2,202,644,583 bp). We compared results from Bcftools/ROH with a rule-based approach implemented in Plink v.1.9 using two different sets of parameters that varied in the size of the sliding window of SNPs (homozyg-window-snp 50 or 500), allowance for heterozygous genotypes (homozyg-window-het 3 or 5), and missing genotypes (homozyg-window-missing 10 or 20). We set the value of all other parameters as follows: homozyg-snp 25, homozyg-window-threshold 0.05, homozyg-kb 100, homozyg-density 50, homozyg-gap 1000. Qualitative results were similar among all methods but Plink tended to break long ROH called with Bcftools into shorter segments and was more sensitive to depth of coverage (supplementary fig. S19, Supplementary Material online); we opted to use results of bcftools/ROH for all downstream analyses.

Long ROH indicate shared ancestry in recent parental generations whereas shorter ROH indicate bottlenecks or founder events in deeper history (Ceballos et al. 2018). We estimated the approximate age for different size classes of ROHs using $g = 100/(2rL)$ (Thompson 2013) where g is expected number generations back to coalescence of the haplotypes that form a ROH, L is the ROH length in Mb, and r is the average recombination rate (0.6 cM/Mb) (Kukekova et al. 2007). Finally, to evaluate the proportion of ROH that arose due to shared versus independent demographic events, we adapted a bash script from (Robinson et al. 2021) to calculate the length of overlapping ROH between pairs of individuals that were identical-by-state. Segments with overlapping ROH were considered identical-by-state when the frequency of fixed differences between them was less than 5e-5.

Deleterious Variation

As most deleterious mutations are assumed to be derived, we inferred the ancestral allele based on consensus of four outgroup reference genomes downloaded from NCBI: arctic fox (GCF_018345385.1), Tibetan sand fox (*Vulpes ferrilata*; GCA_024500485.1), domestic dog (*Canis lupus familiaris*; GCA_000002285.2), and raccoon dog (*Nyctereutes procyonoides*; GCA_905146905.1). We used makeWindows and getFasta in Bedtools2 to split reference genomes into overlapping 70-bp fragments with a sliding step of 10 bp. We converted from fasta to fastq using seqtk (<https://github.com/lh3/seqtk>), which we mapped to the arctic fox genome using BWA mem. We then used bcftools mpileup and call to obtain genotypes for each polymorphic site in our dataset and identified the ancestral allele as the majority allele of all sites where at least three outgroup references mapped. We added the ancestral allele as AA tags to the INFO field of the vcf using vcftools vcf-annotate (Danecek et al. 2011) and rotated genotypes such that the reference allele matched the ancestral allele using vcfilterjdk and a java script from https://github.com/k-hench/test_ancestral_allele.

We focused our analysis of deleterious load on the protein coding exome as amino acid substitutions provide the most straightforward predictions of functional impact. We used SnpEff v.5.1 (Cingolani et al. 2012) to classify the

derived alleles as synonymous, missense, and LoF mutations in coding sequences based on annotation of the arctic fox reference genome (Peng et al. 2021). As multiple transcripts can overlap, we selected the most deleterious annotations for each variant and removed sites with SnpEff warnings that were indicative of mapping or annotation errors. We further divided missense variants into tolerant and deleterious based on scores (deleterious < 0.05) calculated using the SIFT4G (SIFT for genomes) algorithm (Vaser et al. 2016) and a predictive database built according to instructions at https://github.com/pauline-ng/SIFT4G_Create_Genomic_DB. The SIFT approach uses both conservation of sequence homology in related species and amino acid properties to predict the severity of substitutions on protein function (Ng and Henikoff 2003).

We counted the abundance and distribution of derived alleles within individuals to estimate the potential, realized, and total loads of putative deleterious variation. As deleterious alleles are expected to be recessive, the number of homozygous genotypes approximates the realized load. Past studies have equated the potential load with the masked load, or the number of deleterious alleles in heterozygous state. We suggest, however, that the masked load is an incomplete index of the potential load when considering genetic rescue, as gene flow decouples the frequency and genotypes of alleles from their current genotypic state. Instead, we estimated the potential load as the total number of sites with a deleterious allele, regardless of its genotype, as a more appropriate metric of a translocated animal contributing deleterious alleles to the target population. To infer differences in selection, we estimated the total load as the number of deleterious alleles per individual ($2\times$ homozygous + $1\times$ heterozygous). For all metrics, we normalized for varying levels of missing data among individuals following the approach of (Marsden et al. 2016). For example, we computed the normalized number of derived homozygotes as the fraction of derived homozygous genotypes for individual i and mutation class j relative to the total number of callable sites for individual i and mutation class j , multiplied by the number of homozygous derived genotypes in mutation class j averaged across all i individuals.

We estimated population-based indices of genetic load from SFS. We estimated population specific SFS for three populations of large (RM), moderate (ORC), and small (LAS) effective sizes to evaluate how anthropogenic declines affected the frequency distribution of deleterious sites. To facilitate comparison with uneven sample sizes, we sampled without replacement eight alleles (i.e. chromosomes) from each population. We then evaluated differences in average allele frequencies among populations and mutational categories using a two-way ANOVA and Tukey's HSD tests for pairwise differences. We calculated R_{XY} (Do et al. 2014; Xue et al. 2015) as a metric of the relative frequency of derived alleles in a specific mutational category of one population relative to another. To account for population-specific biases, we standardized R_{XY} estimates using a random set of 80,000 intergenic SNPs

expected to drift neutrally and estimated standard errors for R_{XY} by jackknifing estimates with 100 blocks of contiguous SNPs.

To evaluate deleterious variation explicitly in the context of genetic rescue, we calculated pairwise indices of deleterious variation among all individuals. These indices represent how deleterious variation might be distributed in the progeny of the targeted pair. We grouped individuals into candidate recipient and donor populations and focused on three metrics relevant to genetic rescue: capacity of the donor to mask homozygous deleterious alleles in the recipient (number of sites where the recipient was homozygous for a deleterious allele and the donor had at least one ancestral allele), introduction of novel deleterious alleles from the donor (number of sites where donor individual had at least one deleterious allele and recipient had none), and shared deleterious alleles between donors (number of sites homozygous in one donor individual that were also homozygous in a second donor individual). For each combination of populations, we calculated the mean value of all pairwise comparisons. We constructed bootstrap confidence intervals around the mean by randomly resampling with replacement for the same number of times as the number of observed comparisons. We conducted 1,000 bootstrap replicates and applied the 0.025 and 0.975 quantiles to define the 95% confidence interval. To test whether populations yielded significantly different estimates, we randomized the population affiliation of all individuals 1,000 times and recalculated pairwise load indices for each replicate. We then calculated the P -value as the proportion of replicates with a difference in estimates at least as large as the observed value.

Supplementary Material

Supplementary material is available at *Molecular Biology and Evolution* online.

Acknowledgments

We thank J. Akins, P. Alden, G. Green, T. Hiller, R. Mason, J. Perrine, R. Stroeberl, Oregon Department of Fish and Wildlife (J. Bowles), Crater Lake National Park (S. Mohren), California Department of Fish and Wildlife (C. Stermer) for providing the tissue samples used in this study. Critical lab work was provided by S. Vanderzwan and J. Owen-Ramos. Two anonymous reviewers greatly improved this work.

Author Contributions

Cate B. Quinn (Conceptualization, Methodology, Investigation, Visualization, Writing—original draft, Writing—review & editing), Sophie Preckler-Quisquater (Methodology, Writing—review & editing), Michael R. Buchalski (Methodology, Supervision, Writing—review & editing), and Benjamin N. Sacks (Conceptualization, Methodology, Supervision, Writing—review & editing).

Funding

United States Fish and Wildlife Service (agreement No. F20AC00037; B.N.S.). State Wildlife Grant (agreement No. F22AF01912) awarded by the United States Fish and Wildlife Service to California Department of Fish and Wildlife (MRB). Mammalian Conservation Unit, University of Davis, California.

Conflict of Interest

All authors declare that they have no competing interests.

Data Availability

All code used in analysis is available at https://github.com/cbquinn/westernRF_WGS and raw sequence data are archived at the National Center for Biotechnology Information (NCBI) in the Sequence Read Archive under BioProject PRJNA1158265. All data are available in the main text or the [supplementary materials](#).

References

- Alexander DH, Novembre J, Lange K. Fast model-based estimation of ancestry in unrelated individuals. *Genome Res.* 2009;**19**(9):1655–1664. <https://doi.org/10.1101/gr.094052.109>.
- Aubry KB, Statham MJ, Sacks BN, Perrine JD, Wisely SM. Phylogeography of the North American red fox: vicariance in Pleistocene forest refugia. *Mol Ecol.* 2009;**18**(12):2668–2686. <https://doi.org/10.1111/j.1365-294X.2009.04222.x>.
- Beaumont MA, Zhang W, Balding DJ. Approximate Bayesian computation in population genetics. *Genetics.* 2002;**162**(4):2025–2035. <https://doi.org/10.1093/genetics/162.4.2025>.
- Bell DA, Robinson ZL, Funk WC, Fitzpatrick SW, Allendorf FW, Tallmon DA, Whiteley AR. The exciting potential and remaining uncertainties of genetic rescue. *Trends Ecol Evol.* 2019;**34**(12):1070–1079. <https://doi.org/10.1016/j.tree.2019.06.006>.
- Bertorelle G, Raffini F, Bosse M, Bortoluzzi C, Iannucci A, Trucchi E, Morales HE, van Oosterhout C. Genetic load: genomic estimates and applications in non-model animals. *Nat Rev Genet.* 2022;**23**(8):492–503. <https://doi.org/10.1038/s41576-022-00448-x>.
- Blischak PD, Barker MS, Gutenkunst RN. Inferring the demographic history of inbred species from genome-wide SNP frequency data. *Mol Biol Evol.* 2020;**37**(7):2124–2136. <https://doi.org/10.1093/molbev/msaa042>.
- Blum MGB, François O. Non-linear regression models for approximate Bayesian computation. *Stat Comput.* 2010;**20**(1):63–73. <https://doi.org/10.1007/s11222-009-9116-0>.
- Brown JL, Hill DJ, Dolan AM, Carnaval AC, Hayward AM. PaleoClim, high spatial resolution paleoclimate surfaces for global land areas. *Sci Data.* 2018;**5**(1):180254. <https://doi.org/10.1038/sdata.2018.254>.
- Burnham KP, Anderson DR. Multimodel inference: understanding AIC and BIC in model selection. *Sociol Methods Res.* 2004;**33**(2):261–304. <https://doi.org/10.1177/0049124104268644>.
- Ceballos FC, Joshi PK, Clark DW, Ramsay M, Wilson JF. Runs of homozygosity: windows into population history and trait architecture. *Nat Rev Genet.* 2018;**19**(4):220–234. <https://doi.org/10.1038/nrg.2017.109>.
- Center for Biological Diversity. 2024. [accessed 2024 Aug 5]. https://biologicaldiversity.org/species/mammals/Sierra_Nevada_red_fox/pdfs/2024-02-08-Sierra-Nevada-Red-Fox-Petition-Final.pdf.
- Chang CC, Chow CC, Tellier LC, Vattikuti S, Purcell SM, Lee JJ. Second-generation PLINK: rising to the challenge of larger and richer datasets. *Gigascience.* 2015;**4**(1):7. <https://doi.org/10.1186/s13742-015-0047-8>.
- Cingolani P, Platts A, Wang LL, Coon M, Nguyen T, Wang L, Land SJ, Lu X, Ruden DM. A program for annotating and predicting the effects of single nucleotide polymorphisms, SnpEff. *Fly (Austin).* 2012;**6**(2):80–92. <https://doi.org/10.4161/fly.19695>.
- Csilléry K, François O, Blum MGB. ABC: an R package for approximate Bayesian computation (ABC). *Methods Ecol Evol.* 2012;**3**(3):475–479. <https://doi.org/10.1111/j.2041-210X.2011.00179.x>.
- Danecek P, Auton A, Abecasis G, Albers CA, Banks E, DePristo MA, Handsaker RE, Lunter G, Marth GT, Sherry ST, et al. The variant call format and VCFtools. *Bioinformatics.* 2011;**27**(15):2156–2158. <https://doi.org/10.1093/bioinformatics/btr330>.
- Delaneau O, Zagury J-F, Robinson MR, Marchini JL, Dermitzakis ET. Accurate, scalable and integrative haplotype estimation. *Nat Commun.* 2019;**10**(1):5436. <https://doi.org/10.1038/s41467-019-13225-y>.
- Do C, Waples RS, Peel D, Macbeth GM, Tillett BJ, Ovenden JR. Neestimator v2: re-implementation of software for the estimation of contemporary effective population size (Ne) from genetic data. *Mol Ecol Resour.* 2014;**14**(1):209–214. <https://doi.org/10.1111/1755-0998.12157>.
- Dussex N, Morales HE, Gossen C, Dalén L, van Oosterhout C. Purging and accumulation of genetic load in conservation. *Trends Ecol Evol.* 2023;**38**(10):961–969. <https://doi.org/10.1016/j.tree.2023.05.008>.
- Dussex N, van der Valk T, Morales HE, Wheat CW, Díez-del-Molino D, von Seth J, Foster Y, Kutschera VE, Guschanski K, Rhie A, et al. Population genomics of the critically endangered kākāpō. *Cell Genom.* 2021;**1**(1):100002. <https://doi.org/10.1016/j.xgen.2021.100002>.
- Edmonds S. Between a rock and a hard place: evaluating the relative risks of inbreeding and outbreeding for conservation and management. *Mol Ecol.* 2007;**16**(3):463–475. <https://doi.org/10.1111/j.1365-294X.2006.03148.x>.
- Fitzpatrick SW, Mittan-Moreau C, Miller M, Judson JM. Genetic rescue remains underused for aiding recovery of federally listed vertebrates in the United States. *J Hered.* 2023;**114**(4):354–366. <https://doi.org/10.1093/jhered/esad002>.
- Fordham DA, Saltré F, Haythorne S, Wigley TML, Otto-Bliesner BL, Chan KC, Brook BW. PaleoView: a tool for generating continuous climate projections spanning the last 21 000 years at regional and global scales. *Ecography.* 2017;**40**(11):1348–1358. <https://doi.org/10.1111/ecog.03031>.
- Frankham R. Genetic rescue of small inbred populations: meta-analysis reveals large and consistent benefits of gene flow. *Mol Ecol.* 2015;**24**(11):2610–2618. <https://doi.org/10.1111/mec.13139>.
- Frankham R, Ballou JD, Eldridge MDB, Lacy RC, Ralls K, Dudash MR, Fenster CB. Predicting the probability of outbreeding depression. *Conserv Biol.* 2011;**25**(3):465–475. <https://doi.org/10.1111/j.1523-1739.2011.01662.x>.
- Gilpin M. Minimum viable populations: processes of extinction. In: Soulé ME, editor. *Conservation biology: the science of scarcity and diversity*. Sunderland (MA): Sinauer Associates; 1986. p. 19–34.
- Green DS, Martin ME, Matthews SM, Akins JR, Carlson J, Figura P, Hatfield BE, Perrine JD, Quinn CB, Sacks BN, et al. A hierarchical modeling approach to predict the distribution and density of Sierra Nevada Red Fox (*Vulpes vulpes nescator*). *J Mammal.* 2023;**104**(4):820–832. <https://doi.org/10.1093/jmammal/gyad026>.
- Grinnell J, Dixon JS, Linsdale JM. *Fur-bearing mammals of California*. Berkeley (California): University of California Press; 1937.
- Gossen C, Guillaume F, Keller LF, Croll D. Purging of highly deleterious mutations through severe bottlenecks in Alpine ibex. *Nat Commun.* 2020;**11**(1):1001. <https://doi.org/10.1038/s41467-020-14803-1>.
- Gutenkunst RN, Hernandez RD, Williamson SH, Bustamante CD. Inferring the joint demographic history of multiple populations from multidimensional SNP frequency data. *PLoS Genet.* 2009;**5**(10):e1000695. <https://doi.org/10.1371/journal.pgen.1000695>.
- Harris K, Zhang Y, Nielsen R. Genetic rescue and the maintenance of native ancestry. *Conserv Genet.* 2019;**20**(1):59–64. <https://doi.org/10.1007/s10592-018-1132-1>.

- Hatfield BE, Runcie JM, Siemion EA, Quinn CB, Stephenson TR. New detections extend the known range of the state-threatened Sierra Nevada red fox. *Calif Fish Wildl J*. 2021;**107**(CESA Special Issue):438–443. <https://doi.org/10.51492/cfwj.cesai.26>.
- Haubold B, Pfaffelhuber P, Lynch M. mlRho—a program for estimating the population mutation and recombination rates from shotgun-sequenced diploid genomes. *Mol Ecol*. 2010;**19**(Suppl 1):277–284. <https://doi.org/10.1111/j.1365-294X.2009.04482.x>.
- Hedrick PW, Fredrickson R. Genetic rescue guidelines with examples from Mexican wolves and Florida panthers. *Conserv Genet*. 2010;**11**(2):615–626. <https://doi.org/10.1007/s10592-009-9999-5>.
- Hedrick PW, Garcia-Dorado A. Understanding inbreeding depression, purging, and genetic rescue. *Trends Ecol Evol*. 2016;**31**(12):940–952. <https://doi.org/10.1016/j.tree.2016.09.005>.
- Hedrick PW, Robinson JA, Peterson RO, Vucetich JA. Genetics and extinction and the example of Isle Royale wolves. *Anim Conserv*. 2019;**22**(3):302–309. <https://doi.org/10.1111/acv.12479>.
- Jakobsson M, Pearce C, Cronin TM, Backman J, Anderson LG, Barrientos N, Björk G, Coxall H, De Boer A, Mayer LA, et al. Post-glacial flooding of the Bering Land Bridge dated to 11 cal ka BP based on new geophysical and sediment records. *Clim Past*. 2017;**13**(8):991–1005. <https://doi.org/10.5194/cp-13-991-2017>.
- Kardos M, Armstrong EE, Fitzpatrick SW, Hauser S, Hedrick PW, Miller JM, Tallmon DA, Funk WC. The crucial role of genome-wide genetic variation in conservation. *Proc Natl Acad Sci U S A*. 2021;**118**(48):e2104642118. <https://doi.org/10.1073/pnas.2104642118>.
- Kardos M, Taylor HR, Ellegren H, Luikart G, Allendorf FW. Genomics advances the study of inbreeding depression in the wild. *Evol Appl*. 2016;**9**(10):1205–1218. <https://doi.org/10.1111/eva.12414>.
- Karger DN, Conrad O, Böhner J, Kawohl T, Kreft H, Soria-Auza RW, Zimmermann NE, Linder HP, Kessler M. Climatologies at high resolution for the earth's land surface areas. *Sci Data*. 2017;**4**(1):170122. <https://doi.org/10.1038/sdata.2017.122>.
- Kass JM, Muscarella R, Galante PJ, Bohl CL, Pinilla-Buitrago GE, Boria RA, Soley-Guardia M, Anderson RP. ENMeval 2.0: redesigned for customizable and reproducible modeling of species' niches and distributions. *Methods Ecol Evol*. 2021;**12**(9):1602–1608. <https://doi.org/10.1111/2041-210X.13628>.
- Khan A, Patel K, Shukla H, Viswanathan A, van der Valk T, Borthakur U, Nigam P, Zachariah A, Jhala YV, Kardos M, et al. Genomic evidence for inbreeding depression and purging of deleterious genetic variation in Indian tigers. *Proc Natl Acad Sci U S A*. 2021;**118**(49):e2023018118. <https://doi.org/10.1073/pnas.2023018118>.
- Kirkpatrick M, Jarne P. The effects of a bottleneck on inbreeding depression and the genetic load. *Am Nat*. 2000;**155**(2):154–167. <https://doi.org/10.1086/303312>.
- Kleinman-Ruiz D, Lucena-Perez M, Villanueva B, Fernández J, Saveljev AP, Ratkiewicz M, Schmidt K, Galtier N, García-Dorado A, Godoy JA. Purging of deleterious burden in the endangered Iberian lynx. *Proc Natl Acad Sci U S A*. 2022;**119**(11):e2110614119. <https://doi.org/10.1073/pnas.2110614119>.
- Koch EM, Schweizer RM, Schweizer TM, Stahler DR, Smith DW, Wayne RK, Novembre J. De novo mutation rate estimation in wolves of known pedigree. *Mol Biol Evol*. 2019;**36**(11):2536–2547. <https://doi.org/10.1093/molbev/msz159>.
- Krueger F. 2012. [accessed 2024 Jul 5]. Available from: http://www.bioinformatics.babraham.ac.uk/projects/trim_galore/.
- Kukekova AV, Trut LN, Oskina IN, Johnson JL, Temnykh SV, Kharlamova AV, Shepeleva DV, Gulievich RG, Shikhevich SG, Graphodatsky AS, et al. A meiotic linkage map of the silver fox, aligned and compared to the canine genome. *Genome Res*. 2007;**17**(3):387–399. <https://doi.org/10.1101/gr.5893307>.
- Kurland S, Ryman N, Hössjer O, Laikre L. Effects of subpopulation extinction on effective size (Ne) of metapopulations. *Conserv Genet*. 2023;**24**(4):417–433. <https://doi.org/10.1007/s10592-023-01510-9>.
- Kyriazis CC, Robinson JA, Lohmueller KE. Using computational simulations to model deleterious variation and genetic load in natural populations. *Am. Nat.* 2023;**202**(6):737–752. <https://doi.org/10.1086/726736>.
- Kyriazis CC, Wayne RK, Lohmueller KE. Strongly deleterious mutations are a primary determinant of extinction risk due to inbreeding depression. *Evol Lett*. 2021;**5**(1):33–47. <https://doi.org/10.1002/evl3.209>.
- Li H. 2013. Aligning sequence reads, clone sequences and assembly contigs with BWA-MEM, arXiv, arXiv:1303.3997v2, preprint: not peer reviewed
- Li H, Durbin R. Inference of human population history from individual whole-genome sequences. *Nature*. 2011;**475**(7357):493–496. <https://doi.org/10.1038/nature10231>.
- Li H, Handsaker B, Wysoker A, Fennell T, Ruan J, Homer N, Marth G, Abecasis G, Durbin R; 1000 Genome Project Data Processing Subgroup. The sequence alignment/map format and SAMtools. *Bioinformatics*. 2009;**25**(16):2078–2079. <https://doi.org/10.1093/bioinformatics/btp352>.
- Liberg O, Andrén H, Pedersen H-C, Sand H, Sejberg D, Wabakken P, Kesson M, Bensch S. Severe inbreeding depression in a wild wolf (*Canis lupus*) population. *Biol Lett*. 2005;**1**(1):17–20. <https://doi.org/10.1098/rsbl.2004.0266>.
- Luque GM, Vayssade C, Facon B, Guillemaud T, Courchamp F, Fauvergue X. The genetic allee effect: a unified framework for the genetics and demography of small populations. *Ecosphere*. 2016;**7**(7):e01413. <https://doi.org/10.1002/ecs2.1413>.
- Manichaikul A, Mychaleckyj JC, Rich SS, Daly K, Sale M, Chen W-M. Robust relationship inference in genome-wide association studies. *Bioinformatics*. 2010;**26**(22):2867–2873. <https://doi.org/10.1093/bioinformatics/btq559>.
- Marsden CD, Ortega-Del Vecchyo D, O'Brien DP, Taylor JF, Ramirez O, Vilà C, Marques-Bonet T, Schnabel RD, Wayne RK, Lohmueller KE. Bottlenecks and selective sweeps during domestication have increased deleterious genetic variation in dogs. *Proc Natl Acad Sci U S A*. 2016;**113**(1):152–157. <https://doi.org/10.1073/pnas.1512501113>.
- Martin M. Cutadapt removes adapter sequences from high-throughput sequencing reads. *EMBnet J*. 2011;**17**(1):10–12. <https://doi.org/10.14806/ej.17.1.200>.
- Mather N, Traves SM, Ho SYW. A practical introduction to sequentially Markovian coalescent methods for estimating demographic history from genomic data. *Ecol Evol*. 2020;**10**(1):579–589. <https://doi.org/10.1002/ece3.5888>.
- Mathur S, DeWoody JA. Genetic load has potential in large populations but is realized in small inbred populations. *Evol Appl*. 2021;**14**(6):1540–1557. <https://doi.org/10.1111/eva.13216>.
- Narasimhan V, Danecek P, Scally A, Xue Y, Tyler-Smith C, Durbin R. BCFtools/RoH: a hidden Markov model approach for detecting autozygosity from next-generation sequencing data. *Bioinformatics*. 2016;**32**(11):1749–1751. <https://doi.org/10.1093/bioinformatics/btw044>.
- Ng PC, Henikoff S. SIFT: predicting amino acid changes that affect protein function. *Nucleic Acids Res*. 2003;**31**(13):3812–3814. <https://doi.org/10.1093/nar/gkg509>.
- Norén K, Godoy E, Dalén L, Meijer T, Angerbjörn A. Inbreeding depression in a critically endangered carnivore. *Mol Ecol*. 2016;**25**(14):3309–3318. <https://doi.org/10.1111/mec.13674>.
- Novo I, Ordás P, Moraga N, Santiago E, Quesada H, Caballero A. Impact of population structure in the estimation of recent historical effective population size by the software GONE. *Genet Sel Evol*. 2023;**55**(1):86. <https://doi.org/10.1186/s12711-023-00859-2>.
- Obbard ME, Jones JG, Newman R, Booth A, Satterthwaite AJ, Linscombe G. Furbearer harvests in North America. Wild furbearer management and conservation in North America. Ontario, Canada: Ontario Ministry of Natural Resources and the Ontario Trappers Association; 1987. p. 1007–1034.
- Ochoa A, Onorato DP, Roelke-Parker ME, Culver M, Fitak RR. Give and take: effects of genetic admixture on mutation load in endangered Florida panthers. *J Hered*. 2022;**113**(5):491–499. <https://doi.org/10.1093/jhered/esac037>.
- Onorato DP, Cunningham MW, Lotz M, Criffield M, Shindle D, Johnson A, Clemons BCF, Shea CP, Roelke-Parker ME, Johnson

- WE, et al. Multi-generational benefits of genetic rescue. *Sci Rep*. 2024;**14**(1):17519. <https://doi.org/10.1038/s41598-024-67033-6>.
- Ørsted M, Hoffmann AA, Sverrisdóttir E, Nielsen KL, Kristensen TN. Genomic variation predicts adaptive evolutionary responses better than population bottleneck history. *PLoS Genet*. 2019;**15**(6): e1008205. <https://doi.org/10.1371/journal.pgen.1008205>.
- Pečnerová P, Garcia-Erill G, Liu X, Nursyifa C, Waples RK, Santander CG, Quinn L, Frandsen P, Meisner J, Stæger FF, et al. High genetic diversity and low differentiation reflect the ecological versatility of the African leopard. *Curr Biol*. 2021;**31**(9):1862–1871.e5. <https://doi.org/10.1016/j.cub.2021.01.064>.
- Peng Y, Li H, Liu Z, Zhang C, Li K, Gong Y, Geng L, Su J, Guan X, Liu L, et al. Chromosome-level genome assembly of the Arctic fox (*Vulpes lagopus*) using PacBio sequencing and Hi-C technology. *Mol Ecol Resour*. 2021;**21**(6):2093–2108. <https://doi.org/10.1111/1755-0998.13397>.
- Pérez-Pereira N, Caballero A, García-Dorado A. Reviewing the consequences of genetic purging on the success of rescue programs. *Conserv Genet*. 2022;**23**(1):1–17. <https://doi.org/10.1007/s10592-021-01405-7>.
- Perrine JD, Campbell LA, Green GA. Sierra Nevada Red fox (*Vulpes vulpes necator*): A conservation assessment. Vallejo, California: US Department of Agriculture; 2010.
- Péwé TL, Hopkins D. Mammal remains of pre-Wisconsin age in Alaska. In: Hopkins DM, editors. *The bering land bridge*. Palo Alto (California): Stanford University Press; 1967. p. 266–287.
- Phillips SJ, Anderson RP, Dudík M, Schapire RE, Blair ME. Opening the black box: an open-source release of Maxent. *Ecography*. 2017;**40**(7):887–893. <https://doi.org/10.1111/ecog.03049>.
- Pockrandt C, Alzamel M, Iliopoulos CS, Reinert K. GenMap: ultra-fast computation of genome mappability. *Bioinformatics*. 2020;**36**(12): 3687–3692. <https://doi.org/10.1093/bioinformatics/btaa222>.
- Popescu A-A, Huber KT, Paradis E. Ape 3.0: new tools for distance-based phylogenetics and evolutionary analysis in R. *Bioinformatics*. 2012;**28**(11):1536–1537. <https://doi.org/10.1093/bioinformatics/bts184>.
- Purcell S, Neale B, Todd-Brown K, Thomas L, Ferreira MAR, Bender D, Maller J, Sklar P, de Bakker PIW, Daly MJ, et al. PLINK: a tool set for whole-genome association and population-based linkage analyses. *Am J Hum Genet*. 2007;**81**(3):559–575. <https://doi.org/10.1086/519795>.
- Quinlan AR, Hall IM. BEDTools: a flexible suite of utilities for comparing genomic features. *Bioinformatics*. 2010;**26**(6):841–842. <https://doi.org/10.1093/bioinformatics/btq033>.
- Quinn CB, Akins JR, Hiller TL, Sacks BN. Predicting the potential distribution of the Sierra Nevada red fox in the Oregon Cascades. *J Fish Wildl Manag*. 2018;**9**(2):351–366. <https://doi.org/10.3996/082017-JFWM-067>.
- Quinn CB, Alden PB, Sacks BN. Noninvasive sampling reveals short-term genetic rescue in an insular red fox population. *J Hered*. 2019;**110**(5):559–576. <https://doi.org/10.1093/jhered/esz024>.
- Quinn CB, Preckler-Quisquater S, Akins JR, Cross PR, Alden PB, Vanderzwan SL, Stephenson JA, Figura PJ, Green GA, Hiller TL, et al. Contrasting genetic trajectories of endangered and expanding red fox populations in the western U.S. *Heredity* (Edinb). 2022;**129**(2):123–136. <https://doi.org/10.1038/s41437-022-00522-4>.
- Ralls K, Sunnucks P, Lacy RC, Frankham R. Genetic rescue: a critique of the evidence supports maximizing genetic diversity rather than minimizing the introduction of putatively harmful genetic variation. *Biol Conserv*. 2020;**251**:108784. <https://doi.org/10.1016/j.biocon.2020.108784>.
- Rando HM, Farré M, Robson MP, Won NB, Johnson JL, Buch R, Bastounes ER, Xiang X, Feng S, Liu S, et al. Construction of red fox chromosomal fragments from the short-read genome assembly. *Genes* (Basel). 2018;**9**(6):308. <https://doi.org/10.3390/genes9060308>.
- Robinson J, Kyriazis CC, Yuan SC, Lohmueller KE. Deleterious variation in natural populations and implications for conservation genetics. *Annu Rev Anim Biosci*. 2023;**11**(1):93–114. <https://doi.org/10.1146/annurev-animal-080522-093311>.
- Robinson JA, Bowie RCK, Dudchenko O, Aiden EL, Hendrickson SL, Steiner CC, Ryder OA, Mindell DP, Wall JD. Genome-wide diversity in the California condor tracks its prehistoric abundance and decline. *Curr Biol*. 2021;**31**(13):2939–2946.e5. <https://doi.org/10.1016/j.cub.2021.04.035>.
- Robinson JA, Brown C, Kim BY, Lohmueller KE, Wayne RK. Purging of strongly deleterious mutations explains long-term persistence and absence of inbreeding depression in island foxes. *Curr Biol*. 2018;**28**(21):3487–3494.e4. <https://doi.org/10.1016/j.cub.2018.08.066>.
- Robinson JA, Räikkönen J, Vucetich LM, Vucetich JA, Peterson RO, Lohmueller KE, Wayne RK. Genomic signatures of extensive inbreeding in Isle Royale wolves, a population on the threshold of extinction. *Sci Adv*. 2019;**5**(5):eaau0757. <https://doi.org/10.1126/sciadv.aau0757>.
- Sacks BN, Lounsbury ZT, Statham MJ. Nuclear genetic analysis of the red fox across its trans-pacific range. *J Hered*. 2018;**109**(5): 573–584. <https://doi.org/10.1093/jhered/esy028>.
- Sacks BN, Statham MJ, Perrine JD, Wisely SM, Aubry KB. North American montane red foxes: expansion, fragmentation, and the origin of the Sacramento Valley red fox. *Conserv Genet*. 2010;**11**(4):1523–1539. <https://doi.org/10.1007/s10592-010-0053-4>.
- Santiago E, Novo I, Pardiñas AF, Saura M, Wang J, Caballero A. Recent demographic history inferred by high-resolution analysis of linkage disequilibrium. *Mol Biol Evol*. 2020;**37**(12):3642–3653. <https://doi.org/10.1093/molbev/msaa169>.
- Saremi NF, Supple MA, Byrne A, Cahill JA, Coutinho LL, Dalén L, Figueiró HV, Johnson WE, Milne HJ, O'Brien SJ, et al. Puma genomes from North and South America provide insights into the genomic consequences of inbreeding. *Nat Commun*. 2019;**10**(1):4769. <https://doi.org/10.1038/s41467-019-12741-1>.
- Schiffels S, Wang K. MSMC and MSMC2: the multiple sequentially Markovian coalescent. *Statistical population genomics*. 2020. New York, NY: Humana; 2020. p. 147–165.
- Segelbacher G, Bosse M, Burger P, Galbusera P, Godoy JA, Helsen P, Hvilsum C, Iacolina L, Kahric A, Manfrin C, et al. New developments in the field of genomic technologies and their relevance to conservation management. *Conserv Genet*. 2022;**23**(2):217–242. <https://doi.org/10.1007/s10592-021-01415-5>.
- Sierra Nevada Red Fox Conservation Advisory Team. A conservation strategy for the Sierra Nevada Red Fox. Sacramento, USA: California Department of Fish and Wildlife; 2022.
- Sikes RS, Bryan JA II. Institutional animal care and use committee considerations for the use of wildlife in research and education. *ILAR J*. 2016;**56**(3):335–341. <https://doi.org/10.1093/ilar/ilv071>.
- Smeds L, Ellegren H. From high masked to high realized genetic load in inbred Scandinavian wolves. *Mol Ecol*. 2023;**32**(7):1567–1580. <https://doi.org/10.1111/mec.16802>.
- Statham MJ, Edwards CJ, Norén K, Soulsbury CD, Sacks BN. Genetic analysis of European red foxes reveals multiple distinct peripheral populations and central continental admixture. *Quat Sci Rev*. 2018;**197**:257–266. <https://doi.org/10.1016/j.quascirev.2018.08.019>.
- Statham MJ, Murdoch J, Janecka J, Aubry KB, Edwards CJ, Soulsbury CD, Berry O, Wang Z, Harrison D, Pearce M, et al. Range-wide multilocus phylogeography of the red fox reveals ancient continental divergence, minimal genomic exchange and distinct demographic histories. *Mol Ecol*. 2014;**23**(19):4813–4830. <https://doi.org/10.1111/mec.12898>.
- Stoffel MA, Johnston SE, Pilkington JG, Pemberton JM. Genetic architecture and lifetime dynamics of inbreeding depression in a wild mammal. *Nat Commun*. 2021;**12**(1):2972. <https://doi.org/10.1038/s41467-021-23222-9>.
- Szpiech ZA, Xu J, Pemberton TJ, Peng W, Zöllner S, Rosenberg NA, Li JZ. Long runs of homozygosity are enriched for deleterious variation. *Am J Hum Genet*. 2013;**93**(1):90–102. <https://doi.org/10.1016/j.ajhg.2013.05.003>.
- Tapper S, Reynolds J. 1996. The wild fur trade: historical and ecological perspectives. In: Taylor VJ, Dunstone N, editors. *The exploitation of mammal populations*. Dordrecht: Springer Netherlands. p. 28–44.

- Thompson EA. Identity by descent: variation in meiosis, across genomes, and in populations. *Genetics*. 2013;**194**(2):301–326. <https://doi.org/10.1534/genetics.112.148825>.
- Thorpe AS, Stanley AG. Determining appropriate goals for restoration of imperilled communities and species. *J Appl Ecol*. 2011;**48**(2): 275–279. <https://doi.org/10.1111/j.1365-2664.2011.01972.x>.
- van der Valk T, de Manuel M, Marques-Bonet T, Guschanski K. Estimates of genetic load suggest frequent purging of deleterious alleles in small populations. *bioRxiv* 696831. <https://doi.org/10.1101/696831>, 22 April 2021, preprint: not peer reviewed.
- van der Valk T, Díez-del-Molino D, Marques-Bonet T, Guschanski K, Dalén L. Historical genomes reveal the genomic consequences of recent population decline in eastern gorillas. *Curr Biol*. 2019;**29**(1): 165–170.e6. <https://doi.org/10.1016/j.cub.2018.11.055>.
- Van Oosterhout C. Mutation load is the spectre of species conservation. *Nat Ecol Evol*. 2020;**4**(8):1004–1006. <https://doi.org/10.1038/s41559-020-1204-8>.
- van Oosterhout C, Speak SA, Birley T, Bortoluzzi C, Percival-Alwyn L, Urban LH, Groombridge JJ, Segelbacher G, Morales HE. Genomic erosion in the assessment of species extinction risk and recovery potential. *bioRxiv* 507768. <https://doi.org/10.1101/2022.09.13.507768>, 15 September 2022, preprint: not peer reviewed.
- Vaser R, Adusumalli S, Leng SN, Sikic M, Ng PC. SIFT missense predictions for genomes. *Nat Protoc*. 2016;**11**(1):1–9. <https://doi.org/10.1038/nprot.2015.123>.
- Volkman LA, Statham MJ, Mooers AØ, Sacks BN. Genetic distinctiveness of red foxes in the Intermountain West as revealed through expanded mitochondrial sequencing. *J Mammal*. 2015;**96**(2): 297–307. <https://doi.org/10.1093/jmammal/gyv007>.
- Waples RS. Practical application of the linkage disequilibrium method for estimating contemporary effective population size: a review. *Mol Ecol Resour*. 2024;**24**(1):e13879. <https://doi.org/10.1111/1755-0998.13879>.
- Whiteley AR, Fitzpatrick SW, Funk WC, Tallmon DA. Genetic rescue to the rescue. *Trends Ecol Evol*. 2015;**30**(1):42–49. <https://doi.org/10.1016/j.tree.2014.10.009>.
- Wilder AP, Navarro AY, King SND, Miller WB, Thomas SM, Steiner CC, Ryder OA, Shier DM. Fitness costs associated with ancestry to isolated populations of an endangered species. *Conserv Genet*. 2020;**21**(3):589–601. <https://doi.org/10.1007/s10592-020-01272-8>.
- Wilder AP, Supple MA, Subramanian A, Mudide A, Swofford R, Serres-Armero A, Steiner C, Koepfli K-P, Genereux DP, Karlsson EK, et al. The contribution of historical processes to contemporary extinction risk in placental mammals. *Science*. 2023;**380**(6643): eabn5856. <https://doi.org/10.1126/science.abn5856>.
- Wootton E, Robert C, Taillon J, Côté SD, Shafer ABA. Genomic health is dependent on long-term population demographic history. *Mol Ecol*. 2023;**32**(8):1943–1954. <https://doi.org/10.1111/mec.16863>.
- Xue Y, Prado-Martinez J, Sudmant PH, Narasimhan V, Ayub Q, Szpak M, Frandsen P, Chen Y, Yngvadottir B, Cooper DN, et al. Mountain gorilla genomes reveal the impact of long-term population decline and inbreeding. *Science*. 2015;**348**(6231):242–245. <https://doi.org/10.1126/science.aaa3952>.